eLife

Cell Biology
Genetics and Genomics

Calcineurin inhibition enhances *Caenorhabditis elegans* lifespan by defecation defects-mediated calorie restriction and nuclear hormone signaling

Reviewed Preprint
v2 • October 9, 2024
Revised by authors

Reviewed Preprint
v1 • August 25, 2023

Priyanka Das, Alejandro Aballay, Jogender Singh

Department of Biological Sciences, Indian Institute of Science Education and Research, Mohali, India • Department of Genetics, The University of Texas MD Anderson Cancer Center, Houston, USA

Abstract

Calcineurin is a highly conserved calcium/calmodulin-dependent serine/threonine protein phosphatase with diverse functions. Inhibition of calcineurin is known to enhance the lifespan of *Caenorhabditis elegans* through multiple signaling pathways. Aiming to study the role of calcineurin in regulating innate immunity, we discover that calcineurin is required for the rhythmic defecation motor program (DMP) in *C. elegans*. Calcineurin inhibition leads to defects in the DMP, resulting in intestinal bloating, rapid colonization of the gut by bacteria, and increased susceptibility to bacterial infection. We demonstrate that intestinal bloating caused by calcineurin inhibition mimics the effects of calorie restriction, resulting in enhanced lifespan. The TFEB ortholog, HLH-30, is required for lifespan extension mediated by calcineurin inhibition. Finally, we show that the nuclear hormone receptor, NHR-8, is upregulated by calcineurin inhibition and is necessary for the increased lifespan. Our studies uncover a role for calcineurin in the *C. elegans* DMP and provide a new mechanism for calcineurin inhibition-mediated longevity extension.

eLife Assessment

This **important** study reveals insights into how calcineurin influences C. elegans pathogen susceptibility and lifespan through its role in controlling the defecation motor program. The authors provide **convincing** evidence to support a new mechanism through which calcineurin impacts longevity. This work will be of interest to investigators studying host-pathogen interactions and aging in a number of experimental systems.

https://doi.org/10.7554/eLife.89572.2.sa3

Introduction

Interventions that enhance lifespan also impart resistance to multiple stresses (Johnson et al., 2001). Indeed, the positive correlation between improved stress resistance and enhanced lifespan has been exploited to identify long-lived mutants (Castro et al., 2004; Denzel et al., 2014; Johnson et al., 2001; Muñoz and Riddle, 2003; Wang et al., 2004). Among stress responses, innate immunity appears to be a crucial factor for enhanced lifespan (Campos et al., 2021; Fabian et al., 2021; Soo et al., 2023; Xia et al., 2019). However, the correlation between innate immunity and lifespan is not always positive. Interventions that alter lifespan may not modulate innate immunity, and vice-versa (Labed et al., 2018; Naim et al., 2021; Otarigho and Aballay, 2020; Sun et al., 2011). Some signaling pathways also establish a tradeoff between innate immunity and lifespan. Mutants that have improved immunity but reduced lifespan have been identified (Amrit et al., 2019; Otarigho and Aballay, 2021; Ren and Ambros, 2015). Conversely, mutants with enhanced lifespans but declined immune responses have also been discovered (Kawli et al., 2010). Moreover, the genetic pathways for lifespan and immunity could be uncoupled in mutants exhibiting enhanced lifespan and improved immune responses (Alper et al., 2010; Guerrero et al., 2021). Therefore, the relationship between lifespan and innate immunity appears to be complex and remains to be fully understood.

Calcineurin, a conserved protein from yeast to humans, is a calcium/calmodulin-dependent serine/threonine protein phosphatase that is involved in diverse cellular processes and signal transduction pathways (Chen et al., 2022; Hogan et al., 2003; Schulz and Yutzey, 2004; Ulengin-Talkish and Cyert, 2023). Dephosphorylation of substrate proteins by calcineurin affects several cellular pathways, including transcriptional signaling programs (Ulengin-Talkish and Cyert, 2023). Calcineurin regulates the activity of the transcription factors of the nuclear factor of activated T cells (NFAT) family (Hogan et al., 2003). Dephosphorylation of NFATs by calcineurin triggers their nuclear localization and activates immune responses in vertebrates (Herbst et al., 2015; Hogan et al., 2003; Vandewalle et al., 2014). In the nematode *Caenorhabditis elegans*, calcineurin regulates thermotaxis, body size, fertility, and lifespan (Bandyopadhyay et al., 2002; Dong et al., 2007; Kuhara et al., 2002; Lee et al., 2013). Knockdown of the catalytic subunit of calcineurin, *tax-6*, is known to enhance *C. elegans* lifespan via multiple pathways, including autophagy and CREB-regulated transcriptional coactivators (CRTCs) (Dong et al., 2007; Dwivedi et al., 2009; Mair et al., 2011; Tao et al., 2013). However, the role of calcineurin in regulating *C. elegans* response to pathogen infections has not been studied. Because *C. elegans* lacks the NFAT transcription factors (Song et al., 2013), it will be intriguing to study how calcineurin inhibition impacts *C. elegans* innate immunity. These studies could also shed some light on the complex interplay between lifespan and immunity.

In this study, we examined the effect of calcineurin inhibition on *C. elegans* innate immunity. Surprisingly, we found that the knockdown of *tax-6* enhanced the susceptibility of *C. elegans* to bacterial infection despite enhancing lifespan. We discovered that *tax-6* is required for the rhythmic defecation motor program (DMP). The knockdown of *tax-6* resulted in intestinal bloating due to defects in the DMP, which enhanced susceptibility to bacterial infection by increasing gut colonization by bacteria. Intestinal bloating resulted in calorie restriction-like phenotypes, including reduced lipid levels, and led to increased lifespan. We discovered that the TFEB ortholog, HLH-30, is required for calcineurin inhibition-mediated lifespan extension. Moreover, we found that the nuclear hormone receptor, NHR-8, is upregulated by calcineurin inhibition and is necessary for increased lifespan. Our studies uncover a new mechanism for calcineurin inhibition-mediated longevity extension.

Results

Calcineurin knockdown enhances *C. elegans* susceptibility to *Pseudomonas aeruginosa* infection

To understand the role of calcineurin in the innate immune response of *C. elegans*, we examined the survival of a hypomorphic allele of *tax-6*, *tax-6(p675)*, when exposed to the pathogenic bacterium *P. aeruginosa* PA14. Surprisingly, *tax-6(p675)* mutants showed significantly reduced survival on *P. aeruginosa* compared to wild-type N2 animals (**Figure 1A**). Similarly, animals carrying a null allele of *tax-6*, *tax-6(ok2065)*, also exhibited a significant decrease in survival on *P. aeruginosa* compared to N2 animals (**Figure 1B**). In addition, knockdown of *tax-6* by RNA interference (RNAi) increased susceptibility to *P. aeruginosa* relative to control animals (**Figure 1C**). The RNAi effects were specific to *tax-6*, as *tax-6(p675)* mutants did not show further increased susceptibility to *P. aeruginosa* when subjected to *tax-6* RNAi (**Figure 1D**). As reported earlier (Dong et al., 2007; Dwivedi et al., 2009; Mair et al., 2011; Tao et al., 2013), we confirmed that both *tax-6* loss of function and RNAi knockdown led to an increased lifespan on *E. coli* (**Figure 1E**, F). An earlier study demonstrated that calcineurin regulates cAMP response element-binding protein (CREB) and CRTCs to regulate lifespan in *C. elegans* (Mair et al., 2011). The knockdown of the CREB homolog-1 (*crh-1*) and *crtc-1* enhanced lifespan similar to the *tax-6* knockdown (Mair et al., 2011). We investigated whether *crh-1* and *crtc-1* knockdowns also affected *C. elegans* survival on *P. aeruginosa* as severely as *tax-6* knockdown. Interestingly, *crh-1* and *crtc-1* knockdowns did not compromise survival on *P. aeruginosa* as much as *tax-6* knockdown did (**Figure 1**). These findings suggested that, despite the increased lifespan, *tax-6* knockdown animals exhibit markedly enhanced susceptibility to *P. aeruginosa* infection through a mechanism likely independent of *crh-1* and *crtc-1*.

We observed enhanced matricidal hatching in *tax-6* knockdown animals on *P. aeruginosa*. Therefore, we asked whether the enhanced susceptibility of *tax-6* knockdown animals to *P. aeruginosa* was because of enhanced matricidal hatching. To this end, we studied the effects of *tax-6* knockdown in *fer-1(b232)* temperature-sensitive mutants. When grown at 25°C, *fer-1(b232)* animals have unfertilized oocytes (Argon and Ward, 1980), thus eliminating the possibility of matricidal hatching. As shown in **Figure 1G**, even in the absence of matricidal hatching, *fer-1(b232)* animals exhibited reduced survival on *P. aeruginosa* following *tax-6* knockdown, indicating that the increased susceptibility is not due to enhanced matricidal hatching. Moreover, *fer-1(b232)* animals showed an extended lifespan on *E. coli* when *tax-6* was knocked down (**Figure 1H**). These results suggested that *tax-6* knockdown leads to both increased lifespan and enhanced susceptibility to pathogen infection.

We then explored whether the increased susceptibility to bacterial infection following *tax-6* knockdown was mediated by any known *C. elegans* innate immunity pathways, including the MAP kinase pathway mediated by NSY-1/SEK-1/PMK-1 (Kim et al., 2002), the MLK-1/MEK-1/KGB-1 c-Jun kinase pathway (Kim et al., 2004), the TGF-β/DBL-1 pathway (Mallo et al., 2002), and the bZIP transcription factor ZIP-2 pathway (Estes et al., 2010). In mutants deficient in each of these pathways, *tax-6* knockdown further increased susceptibility to *P. aeruginosa* (**Figure 2A-D**). The knockdown of *tax-6* appeared to have a more pronounced effect in *pmk-1(km25)* mutants than in other mutants, suggesting that inhibition of *tax-6* might exacerbate the adverse effects observed in *pmk-1(km25)* mutants. Additionally, the increased susceptibility to *P. aeruginosa* seen in *tax-6* knockdown animals was independent of the FOXO transcription factor DAF-16 (**Figure 2E**). Thus, the enhanced susceptibility to *P. aeruginosa* resulting from *tax-6* knockdown appears to operate independently of established *C. elegans* innate immunity pathways.

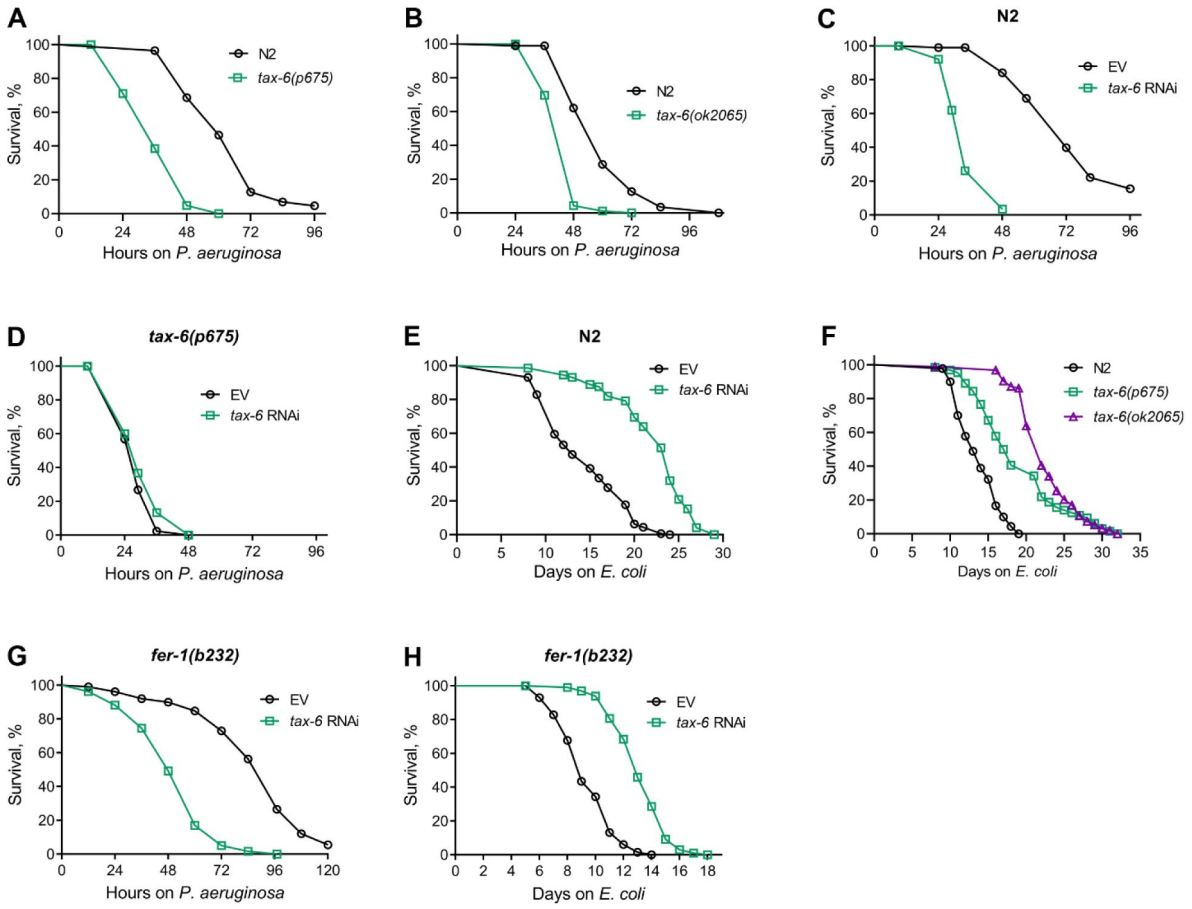

Figure 1

Calcineurin knockdown enhances *C. elegans* susceptibility to *P. aeruginosa*

(A) Representative survival plots of N2 and *tax-6(p675)* animals on *P. aeruginosa* PA14 at 25°C. The animals were grown on *E. coli* OP50 at 20°C until 1-day-old adults before transferring to *P. aeruginosa* PA14 at 25°C. p<0.001.
(B) Representative survival plots of N2 and *tax-6(ok2065)* animals on *P. aeruginosa* PA14 at 25°C. The animals were grown on *E. coli* OP50 at 20°C until 1-day-old adults before transferring to *P. aeruginosa* PA14 at 25°C. p<0.001.
(C) Representative survival plots of N2 animals on *P. aeruginosa* PA14 at 25°C after treatment with the empty vector (EV) control and *tax-6* RNAi. p<0.001.
(D) Representative survival plots of *tax-6(p675)* animals on *P. aeruginosa* PA14 at 25°C after treatment with the EV control and *tax-6* RNAi. n.s., nonsignificant.
(E) Representative survival plots of N2 animals grown on bacteria for RNAi against *tax-6* along with the EV control at 20°C. Day 0 represents young adults. p<0.001.
(F) Representative survival plots of N2, *tax-6(p675)*, and *tax-6(ok2065)* animals grown on *E. coli* OP50 at 20°C. Day 0 represents young adults. p<0.001 for *tax-6(p675)* and *tax-6(ok2065)* compared to N2.
(G) Representative survival plots of *fer-1(b232)* animals on *P. aeruginosa* PA14 at 25°C after treatment with the EV control and *tax-6* RNAi at 25°C. p<0.001.
(H) Representative survival plots of *fer-1(b232)* animals grown on bacteria for RNAi against *tax-6* along with the EV control at 25°C. The animals were developed at 25°C. Day 0 represents young adults. p<0.001. For all panels, n = 3 biological replicates; animals per condition per replicate > 60.

Calcineurin is required for the *C. elegans* defecation motor program (DMP)

To understand why *tax-6* knockdown animals had enhanced susceptibility to *P. aeruginosa* infection, we studied the colonization of the intestine of *tax-6* RNAi animals by *P. aeruginosa*. Knockdown of *tax-6* led to enhanced intestinal colonization by *P. aeruginosa* compared to the control animals (**Figure 2A, B**). Similarly, *tax-6(ok2065)* and *tax-6(p675)* animals also showed increased intestinal colonization by *P. aeruginosa* compared to N2 animals (**Figure 2C, D** and **Figure 3A, B**). Animals with bloated intestinal lumens exhibit enhanced bacterial colonization of the gut, an improved lifespan, and an increased susceptibility to pathogens (Kumar et al., 2019; Singh and Aballay, 2019a). Because *tax-6* knockdown animals displayed all of these phenotypes, we asked whether *tax-6* knockdown led to the bloating of the intestinal lumen. Indeed, we found that *tax-6* knockdown resulted in bloated intestinal lumens (**Figure 2E, F**).

Intestinal bloating could result from either defects in pharyngeal pumping (Kumar et al., 2019) or defects in the defecation motor program (DMP) (Singh and Aballay, 2019a). We found that *tax-6* knockdown did not affect the pharyngeal pumping rate (**Figure 4A**). This prompted us to explore whether calcineurin is necessary for the DMP. The *C. elegans* DMP is a highly coordinated rhythmic behavior required for the regular expulsion of intestinal contents, occurring approximately once per minute. The DMP involves a series of muscle contractions, including posterior body muscle contraction (pBoc), anterior body muscle contraction (aBoc), and expulsion muscle contraction (EMC), to release intestinal contents (Thomas, 1990). When we counted expulsion events over a 20-minute period, we found that *tax-6* knockdown animals had a drastically reduced number of expulsion events (**Figure 2G**). The DMP-defect phenotype had low penetrance in *tax-6(p675)* mutants, which exhibited both regular and irregular DMPs (**Figure 4B**). At the 1-day-old adult stage, about 36% of *tax-6(p675)* animals showed irregular and slowed DMP, while the remainder had regular DMP (**Figure 2H**), suggesting that *tax-6(p675)* is a weak allele. The fraction of the animals with irregular DMP appeared to increase with age, indicating that this phenotype might be age-dependent. This may also explain why *tax-6(p675)* animals were reported to have a normal defecation cycle in an earlier study (Lee et al., 2005).

Next, we investigated whether the reduced number of expulsion events was due to regular intervals with longer cycle lengths or if rhythmicity was entirely disrupted upon *tax-6* knockdown. To assess this, we obtained ethograms of the DMP for N2 animals grown on control and *tax-6* RNAi. While animals on control RNAi displayed regular cycles of pBoc, aBoc, and EMC, the *tax-6* RNAi animals exhibited disrupted rhythmicity (**Figure 3A** and **Figure 5**). Most *tax-6* knockdown animals lacked the pBoc and aBoc steps and had sporadic expulsion events. Isolated pBoc events were occasionally observed, indicating a complete loss of rhythmicity in *tax-6* knockdown animals. Ethograms for *tax-6(ok2065)* animals also showed disrupted rhythmicity (**Figure 3B** and **Figure 6**). Although the number of expulsion events appeared higher in *tax-6(ok2065)* animals compared to *tax-6* RNAi animals (**Figure 5** and S6), these expulsion events seemed superficial, releasing little to no gut content. This suggested slow movement of gut content in *tax-6(ok2065)* animals, leading to constipation and intestinal bloating. We examined gut content movement by measuring the clearance of blue dye (erioglaucine disodium salt) from the gut. The clearance was significantly slower in *tax-6(ok2065)* animals compared to N2 animals (**Figure 3C**), indicating impaired gut content movement due to the loss of *tax-6*. Similarly, *tax-6* knockdown animals also showed significantly slowed gut content movement (**Figure 3D**).

We then explored whether the disruption of DMP rhythmicity due to *tax-6* knockdown affected *P. aeruginosa* responses similarly to longer but regular DMP cycles. To do this, we studied *P. aeruginosa* colonization in *clk-1(qm30)* and *isp-1(qm150)* mutants, which have regular but extended DMP cycles (Feng et al., 2001; Wong et al., 1995). Interestingly, both *clk-1(qm30)* and *isp-1(qm150)* mutants showed significantly reduced intestinal colonization by *P. aeruginosa*

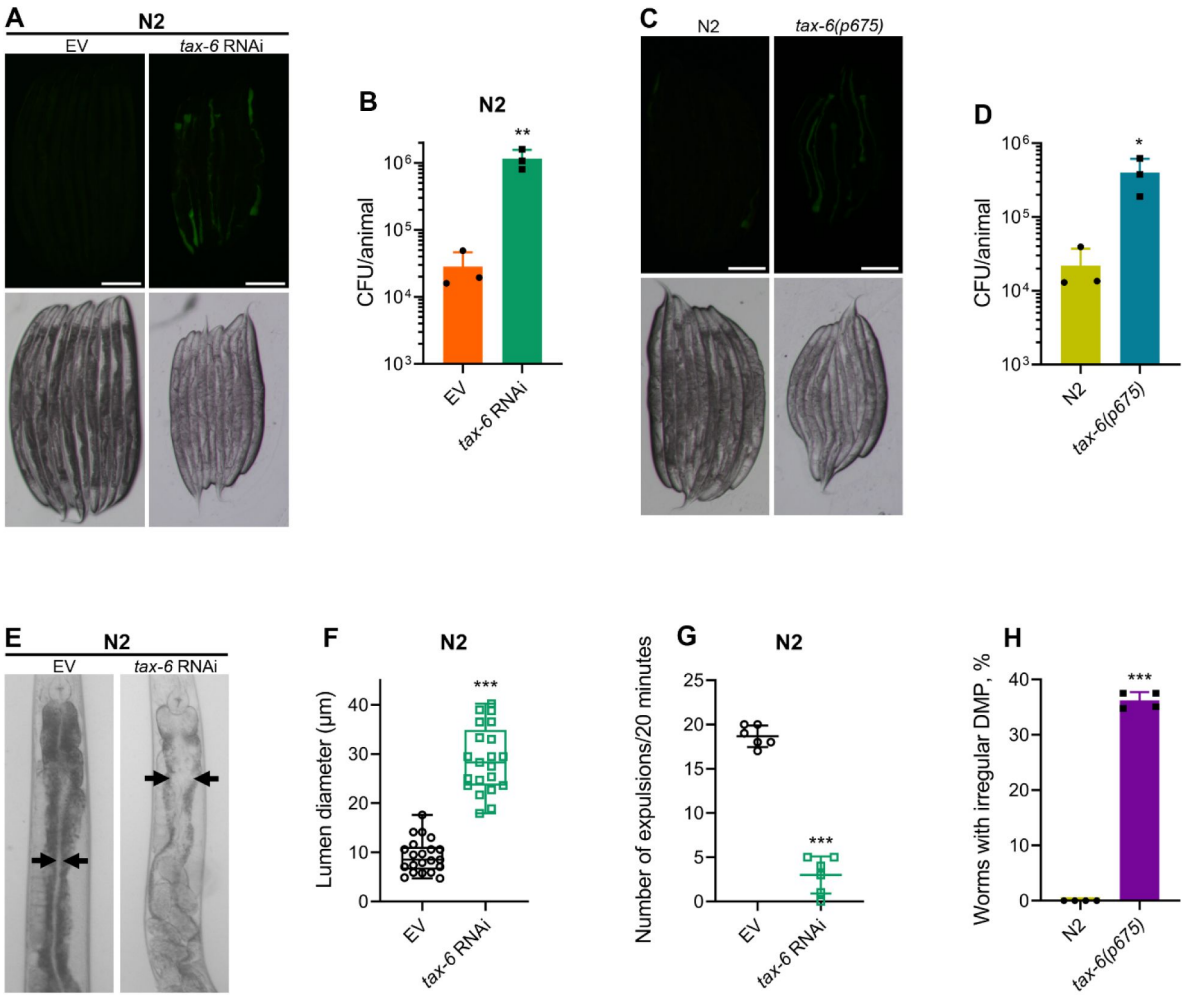

Figure 2

Calcineurin is required for the *C. elegans* defecation motor program (DMP)

(A) Representative fluorescence (top) and the corresponding brightfield (bottom) images of N2 animals incubated on *P. aeruginosa*-GFP for 6 hours at 25°C after growth on the empty vector (EV) control and *tax-6* RNAi bacteria. Scale bar = 200 µm.
(B) Colony-forming units (CFU) per animal of N2 worms incubated on *P. aeruginosa*-GFP for 6 hours at 25°C after growth on the EV control and *tax-6* RNAi bacteria. **p < 0.01 via the *t*-test (n = 3 biological replicates).
(C) Representative fluorescence (top) and the corresponding brightfield (bottom) images of N2 and *tax-6(p675)* animals incubated on *P. aeruginosa*-GFP for 6 hours at 25°C after growth on *E. coli* OP50 at 20°C. Scale bar = 200 µm.
(D) CFU per animal of N2 and *tax-6(p675)* worms incubated on *P. aeruginosa*-GFP for 6 hours at 25°C after growth on *E. coli* OP50 at 20°C. *p < 0.05 via the *t*-test (n = 3 biological replicates).
(E) Representative photomicrographs of N2 animals grown on the EV control and *tax-6* RNAi bacteria at 20°C until 1-day-old adults. Arrows point to the border of the intestinal lumen.
(F) Quantification of the diameter of the intestinal lumen of N2 animals grown on the EV control and *tax-6* RNAi bacteria at 20°C until 1-day-old adults. ***p<0.001 via the *t*-test (n = 21 worms each).
(G) The number of expulsion events observed in 20 minutes in 1-day-old adult N2 animals grown on the EV control and *tax-6* RNAi bacteria at 20°C. ***p<0.001 via the *t*-test (n = 6 worms each).
(H) Percent of 1-day-old adult worms having irregular DMP. ***p<0.001 via the *t*-test (n = 4 biological replicates).

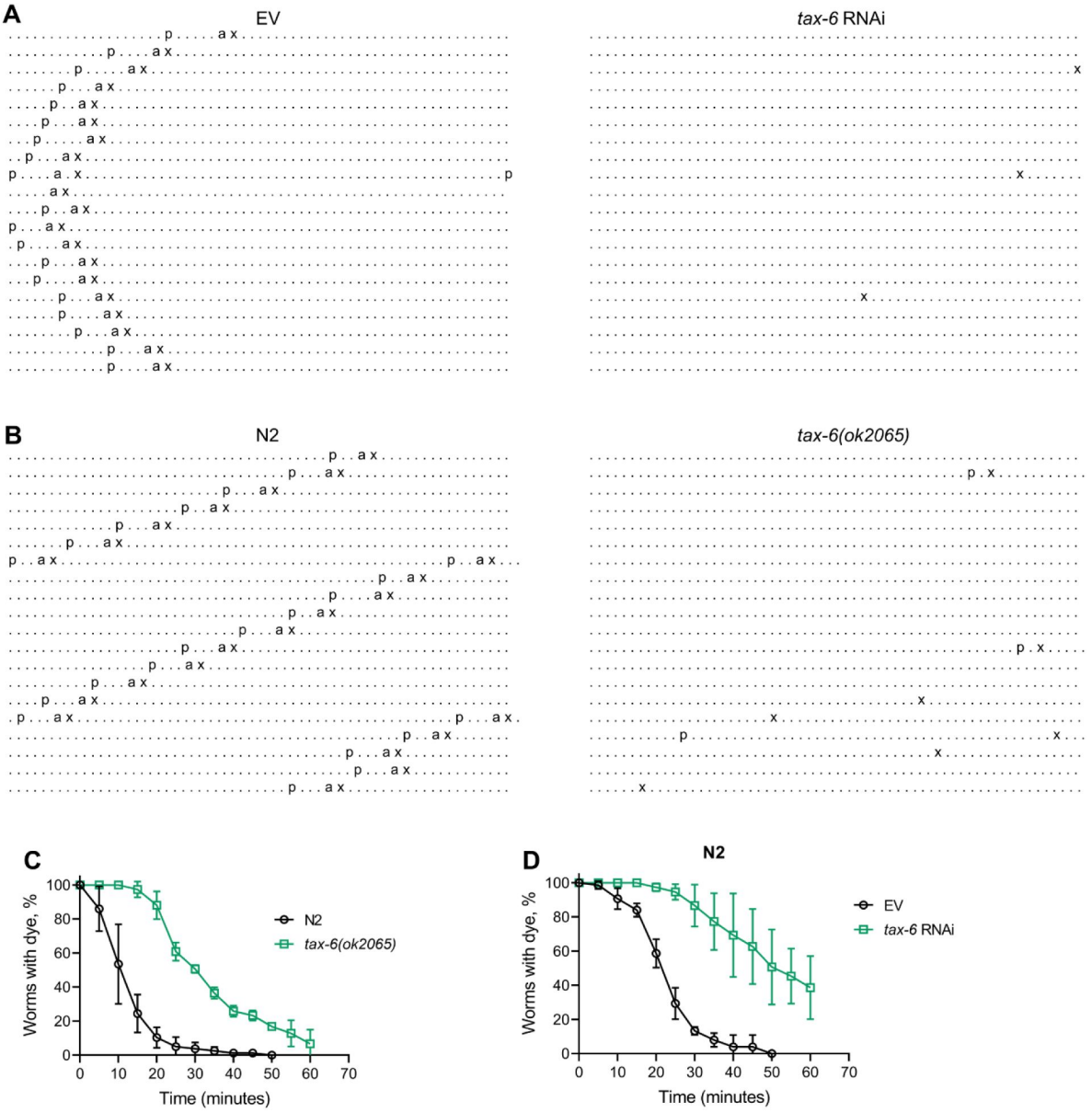

Figure 3

Calcineurin inhibition disrupts the *C. elegans* defecation motor program (DMP)

(A) Representative DMP ethograms of N2 animals after growth on the empty vector (EV) control and *tax-6* RNAi bacteria till 1-day-old stage. Each dot represents a second, and each row represents a minute. 'p', 'a', and 'x' represent posterior body-wall muscle contraction, anterior body-wall muscle contraction, and expulsion muscle contraction, respectively.
(B) Representative DMP ethograms of N2 and *tax-6(ok2065)* animals after their growth on *E. coli* OP50 at 20°C till the 1-day-old adult stage.
(C) Plots of the change in the percent of animals with blue dye in their gut with time for 1-day-old adult N2 and *tax-6(ok2065)* animals (n = 3 biological replicates).
(D) Plots of the change in the percent of animals with blue dye in their gut with time for 1-day-old adult N2 animals grown on EV control and *tax-6* RNAi bacteria (n = 3 biological replicates).

compared to N2 animals (**Figure 7A-D**). This reduced colonization could be attributed to their significantly decreased pharyngeal pumping rates (Wong et al., 1995; Yee et al., 2014), suggesting a lower intake of bacterial food in these mutants. While the survival of *clk-1(qm30)* animals on *P. aeruginosa* was comparable to N2 animals (**Figure 7E**), *isp-1(qm150)* animals exhibited significantly improved survival (**Figure 7F**). Conversely, knockdown of *flr-1*, *nhx-2*, and *pbo-1* in N2 animals resulted in significantly reduced survival on *P. aeruginosa* compared to control RNAi (**Figure 7G**). Knockdown of these genes causes complete disruption of DMP rhythmicity, increasing gut colonization by *P. aeruginosa* (Singh and Aballay, 2019a). Overall, these findings demonstrated that calcineurin is crucial for maintaining the DMP ultradian clock, and its inhibition increases susceptibility to *P. aeruginosa* by disrupting the DMP.

Calcineurin inhibition enhances lifespan via DMP defects-induced calorie restriction

Defects in the *C. elegans* DMP lead to reduced nutrient absorption, resulting in decreased intestinal fat levels (Sheng et al., 2015). We investigated whether *tax-6* knockdown similarly reduces fat levels. To test this, we performed oil-red-O (ORO) staining on *tax-6* RNAi animals. The knockdown of *tax-6* significantly reduced fat levels (**Figure 4A**, B). Next, we examined whether the reduced fat levels in *tax-6* knockdown animals mimic calorie restriction-like phenotypes. Calorie restriction is known to upregulate the expression of the FoxA transcription factor PHA-4 (Panowski et al., 2007). Consistent with this, *tax-6* knockdown also resulted in the upregulation of *pha-4* expression levels (**Figure 4C**). Because calorie restriction enhances lifespan (Kaeberlein et al., 2006; Lakowski and Hekimi, 1998; Panowski et al., 2007), we explored whether calcineurin inhibition could similarly increase lifespan through calorie restriction mechanisms. The knockdown of *tax-6* in the genetic model of calorie restriction, *eat-2(ad465)* (Lakowski and Hekimi, 1998), did not increase the lifespan (**Figure 4D**).

Since *eat-2(ad465)* animals consume fewer bacteria, it is possible that their feeding-based RNAi efficiency is reduced, leading to a lack of responsiveness to *tax-6* RNAi. To assess RNAi efficiency in *eat-2(ad465)* animals, we exposed them to *act-5* and *bli-3* RNAi, which are known to cause developmental arrest and a blistered cuticle, respectively (Gahlot and Singh, 2024). Similar to N2 animals, *eat-2(ad465)* mutants were sensitive to the toxic effects of *act-5* and *bli-3* knockdown (**Figure 8**), indicating that *eat-2(ad465)* animals are not defective in RNAi. To further confirm that calcineurin inhibition enhances lifespan via calorie restriction, we examined the lifespan of *eat-2(ad465);tax-6(ok2065)* double mutants. While *eat-2(ad465)* animals displayed increased lifespan compared to N2 controls, *eat-2(ad465);tax-6(ok2065)* double mutants had a lifespan similar to *tax-6(ok2065)* animals (**Figure 4E**). These results suggested that calcineurin inhibition promotes lifespan extension through calorie restriction mechanisms.

The mechanisms of lifespan enhancement by dietary or calorie restriction are complex and involve several different downstream pathways (Chamoli et al., 2014; Greer and Brunet, 2009; Hansen et al., 2008). Further, different pathways are operational under different dietary regimens (Greer and Brunet, 2009). Therefore, we investigated the involvement of pathways associated with calorie restriction-mediated lifespan extension in response to calcineurin inhibition. Specifically, we analyzed the interactions of the AMP-activated kinase, *aak-2* (Greer and Brunet, 2009), the mTOR pathway, *raga-1* (Robida-Stubbs et al., 2012; Zhang et al., 2019), ribosomal S6 kinase, *rsks-1* (Chen et al., 2009; Selman et al., 2009; Zhang et al., 2019), the FOXO transcription factor, *daf-16* (Greer and Brunet, 2009), and the nuclear hormone receptor, *nhr-49* (Chamoli et al., 2014) with calcineurin inhibition in regulating lifespan. Mutants defective in *aak-2* appeared to have only a partial increase in lifespan upon calcineurin inhibition (**Figure 4F**). In contrast, loss-of-function mutants of *raga-1*, *rsks-1*, *daf-16*, and *nhr-49* exhibited enhanced lifespan upon calcineurin inhibition (**Figure 4G-J**).

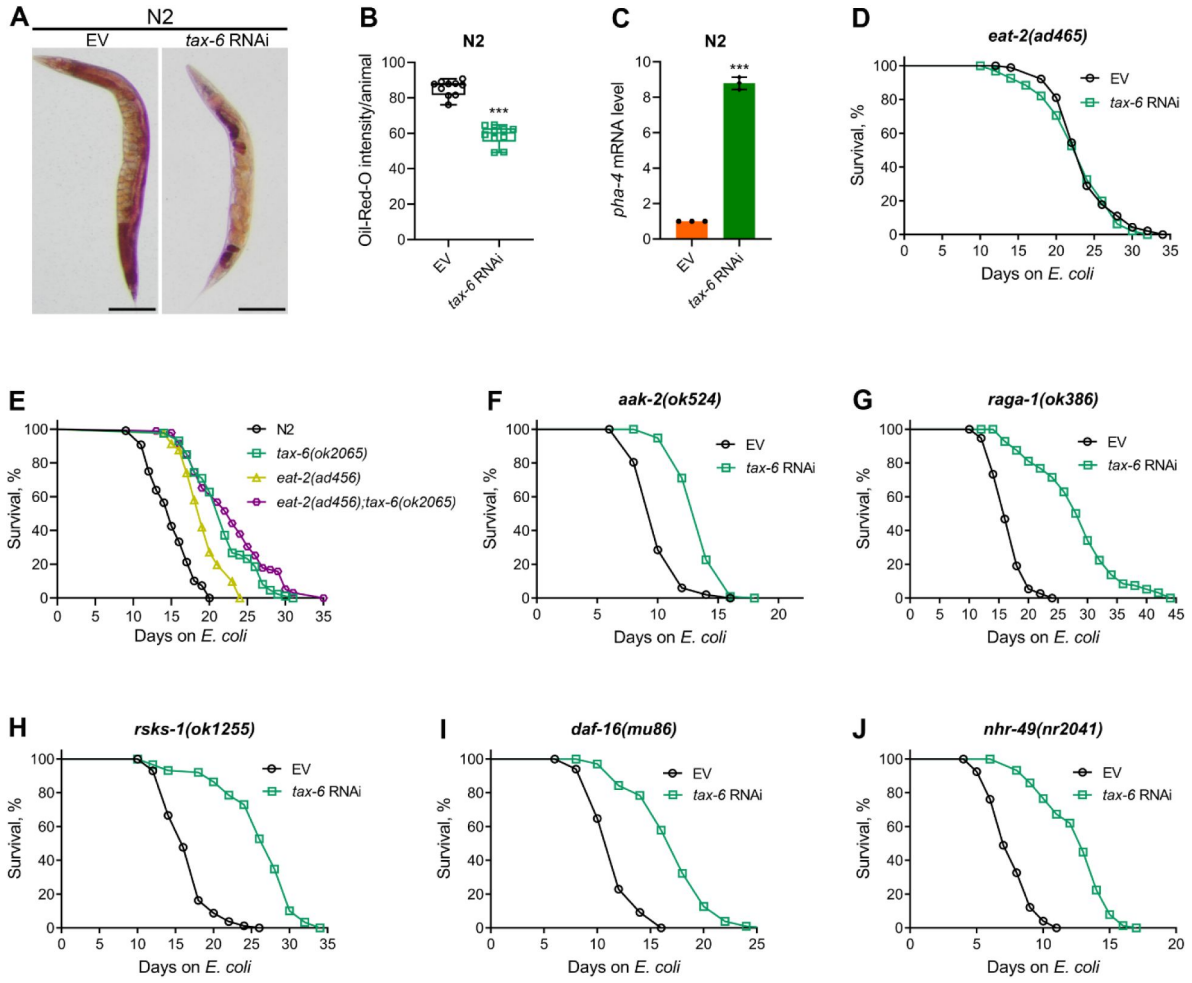

Figure 4

Calcineurin knockdown enhances lifespan via DMP defects-mediated calorie restriction

(A) Representative photomicrographs of oil-red-O (ORO) stained 1-day-old adult N2 animals grown on the empty vector (EV) control and *tax-6* RNAi bacteria at 20°C. Scale bar = 200 µm.
(B) Quantification of ORO intensity per animal of 1-day-old adult N2 animals grown on the EV control and *tax-6* RNAi bacteria at 20°C. The values are area normalized for each animal. ***p<0.001 via the *t*-test (n = 10 worms each).
(C) Quantitative reverse transcription-PCR (qRT-PCR) for *pha-4* mRNA levels in N2 animals grown on the EV control and *tax-6* RNAi bacteria at 20°C until 1-day-old adults. ***p < 0.001 (n = 3 biological replicates).
(D) Representative survival plots of *eat-2(ad465)* animals grown on the bacteria for RNAi against *tax-6* along with the EV control at 20°C. Day 0 represents young adults. n.s., nonsignificant (n = 3 biological replicates; animals per condition per replicate > 80).
(E) Representative survival plots of N2, *tax-6(ok2065)*, *eat-2(ad465)*, and *eat-2(ad465);tax-6(ok2065)* animals grown on *E. coli* OP50 at 20°C. Day 0 represents young adults. p<0.001 for *tax-6(ok2065)*, *eat-2(ad465)*, and *eat-2(ad465);tax-6(ok2065)* compared to N2. p<0.05 for *eat-2(ad465);tax-6(ok2065)* compared to *tax-6(ok2065)* (n = 3 biological replicates; animals per condition per replicate > 65).
(F-J) Representative survival plots of *aak-2(ok524)* (E), *raga-1(ok386)* (F), *rsks-1(ok1255)* (G), *daf-16(mu86)* (H), and *nhr-49(nr2041)* (I) animals grown on the bacteria for RNAi against *tax-6* along with the EV control at 20°C. Day 0 represents young adults. p<0.001 for all the plots (n = 3 biological replicates; animals per condition per replicate > 60).

Calcineurin knockdown enhances lifespan via HLH-30 and NHR-8

To further investigate longevity pathways regulated by calorie restriction that may enhance lifespan downstream of calcineurin inhibition, we examined the role of the TFEB ortholog HLH-30. HLH-30 is essential for the starvation response and triggers lipid depletion under nutrient-deprived conditions (O'Rourke and Ruvkun, 2013). Knockdown of *tax-6* did not extend the lifespan of *hlh-30(tm1978)* animals (**Figure 5A**), indicating that HLH-30 is required for the increased lifespan observed with calcineurin inhibition. To determine whether HLH-30 is necessary for DMP defect-mediated lifespan extension, we assessed the lifespan of *hlh-30(tm1978)* animals upon knockdown of *flr-1*, *nhx-2*, and *pbo-1*. Knockdown of these genes did not alter the lifespan of *hlh-30(tm1978)* animals compared to control RNAi (**Figure 5A**), except for a slight increase in lifespan with *nhx-2* knockdown. The *hlh-30(tm1978)* animals were found to be sensitive to RNAi (**Figure 9**), suggesting that the lack of lifespan change with *tax-6*, *flr-1*, and *pbo-1* RNAi was not due to reduced RNAi efficiency in *hlh-30(tm1978)* animals. Additionally, we confirmed that *tax-6* knockdown caused DMP defects and intestinal bloating in *hlh-30(tm1978)* animals (**Figure 10A-C**). We also explored whether HLH-30 affected fat depletion due to DMP defects. The ORO levels declined significantly in *hlh-30(tm1978)* animals upon the knockdown of *tax-6* and other DMP-regulating genes (**Figure 5B**, C). The reduction in ORO levels was less pronounced in *tax-6* knockdown animals compared to those with other DMP-regulating gene knockdowns.

Steroid hormone signaling mediated by NHR-8 is known to regulate lifespan extension under calorie restriction (Thondamal et al., 2014). We tested whether NHR-8 was necessary for lifespan extension induced by calcineurin inhibition. Indeed, *tax-6* knockdown did not extend the lifespan of *nhr-8(ok186)* animals (**Figure 5D**). While the specific ligands of NHR-8 are not well-defined (Magner et al., 2013), steroid hormones produced by the cytochrome P450 enzyme DAF-9 have been shown to enhance lifespan via NHR-8 under calorie restriction (Thondamal et al., 2014). Therefore, we investigated whether DAF-9 mediated the enhanced lifespan downstream of calcineurin inhibition. We found that *tax-6* knockdown enhanced the lifespan of *daf-9(rh50)* animals (**Figure 5E**), indicating that DAF-9-produced steroid hormones were not required for lifespan increment by calcineurin inhibition. We also examined the lifespan of *nhr-8(ok186)* animals upon knockdown of *flr-1*, *nhx-2*, and *pbo-1*. Knockdown of these genes did not affect the lifespan of *nhr-8(ok186)* animals compared to control RNAi (**Figure 5D**). As with *hlh-30(tm1978)* animals, the lack of lifespan change in *nhr-8(ok186)* animals was not due to RNAi insensitivity, as they were responsive to RNAi (**Figure 9**). Furthermore, *tax-6* knockdown resulted in DMP defects in *nhr-8(ok186)* animals (**Figure 10D**). We investigated whether NHR-8 influenced fat depletion upon DMP defects. A significant reduction in fat levels was observed in *nhr-8(ok186)* animals upon knockdown of *tax-6*, *flr-1*, *nhx-2*, and *pbo-1* (**Figure 5F**, G), suggesting that NHR-8 functions downstream of or in parallel with fat depletion.

Since calorie restriction can enhance the expression of genes that promote lifespan, such as *pha-4* (Panowski et al., 2007), we examined whether *tax-6* knockdown modulates *nhr-8* mRNA levels. We observed a significant increase in *nhr-8* mRNA levels following *tax-6* knockdown (**Figure 5H**). To determine whether this upregulation was due to intestinal bloating, we assessed *nhr-8* mRNA levels in *flr-1*, *nhx-2*, and *pbo-1* knockdown animals. Knockdown of these genes also increased *nhr-8* mRNA levels (**Figure 5H**), indicating that intestinal bloating induces *nhr-8* upregulation. Thus, calcineurin inhibition likely enhances lifespan via NHR-8 by increasing its expression.

Given that HLH-30 and NHR-8 are essential for lifespan extension upon calcineurin inhibition, we investigated whether these pathways also influence survival in response to *P. aeruginosa* infection following calcineurin knockdown. Both *hlh-30(tm1978)* and *nhr-8(ok186)* animals showed significantly reduced survival upon *tax-6* RNAi (**Figure 6A, B**). These findings suggested that the

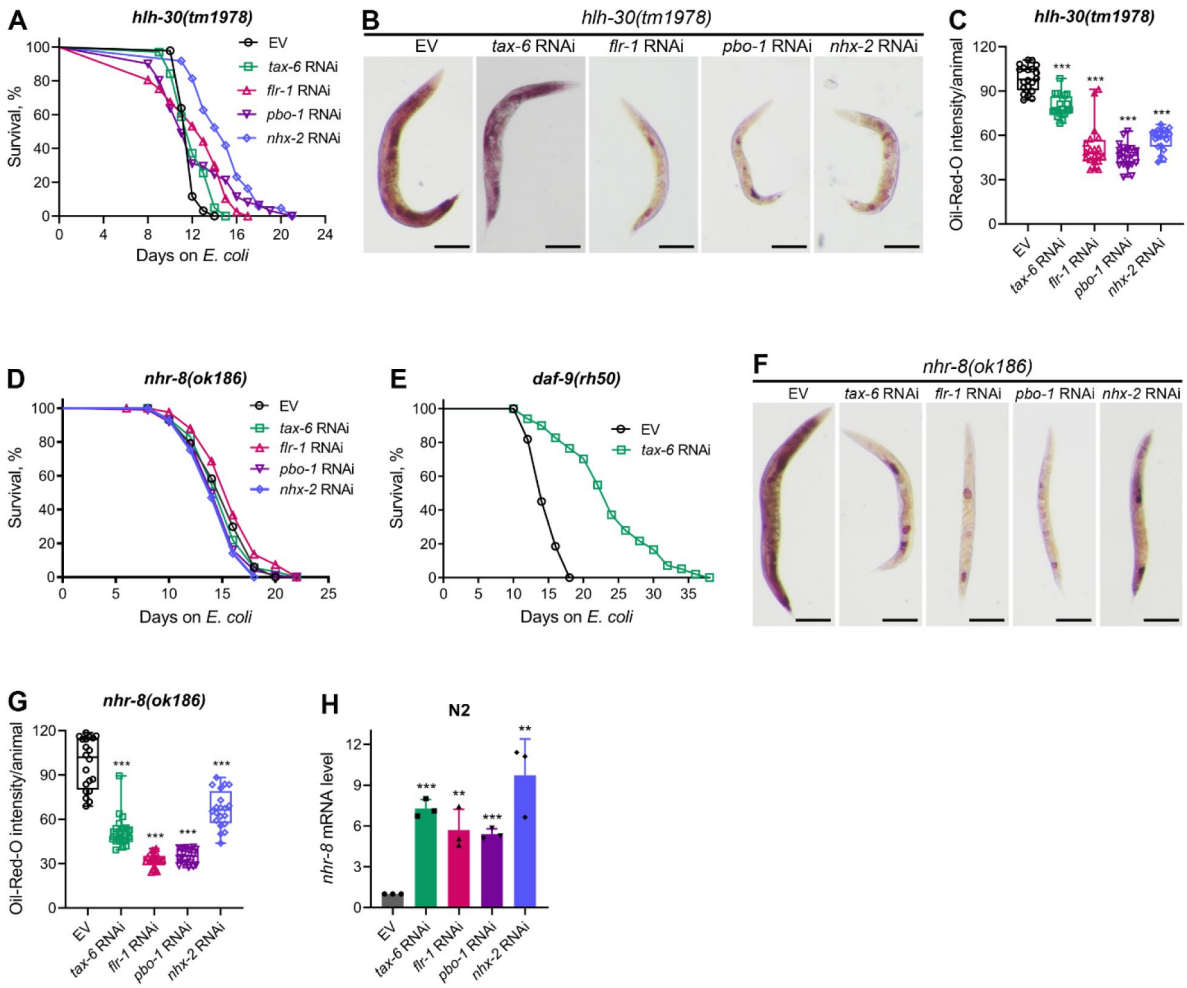

Figure 5

Calcineurin inhibition enhances lifespan via HLH-30 and NHR-8

(A) Representative survival plots of *hlh-30(tm1978)* animals grown on bacteria for RNAi against *tax-6*, *flr-1*, *pbo-1*, and *nhx-2* along with the empty vector (EV) control at 20°C. Day 0 represents young adults. p values for *tax-6*, *flr-1*, *pbo-1*, and *nhx-2* compared to EV are <0.01, <0.001, nonsignificant, and <0.001, respectively (n = 3 biological replicates; animals per condition per replicate > 60).
(B) Representative photomicrographs of oil-red-O (ORO) stained 1-day-old adult *hlh-30(tm1978)* animals grown on the EV control, *tax-6*, *flr-1*, *pbo-1*, and *nhx-2* RNAi bacteria at 20°C. Scale bar = 200 µm.
(C) Quantification of ORO intensity per animal of 1-day-old adult *hlh-30(tm1978)* animals grown on the EV control, *tax-6*, *flr-1*, *pbo-1*, and *nhx-2* RNAi bacteria at 20°C. The values are area normalized for each animal. ***p<0.001 via the *t*-test (n = 20 worms each).
(D) Representative survival plots of *nhr-8(ok186)* animals grown on bacteria for RNAi against *tax-6*, *flr-1*, *pbo-1*, and *nhx-2* along with the EV control at 20°C. Day 0 represents young adults. p values for *tax-6*, *flr-1*, *pbo-1*, and *nhx-2* compared to EV are nonsignificant, <0.05, nonsignificant, and <0.05, respectively (n = 3 biological replicates; animals per condition per replicate > 70).
(E) Representative survival plots of *daf-9(rh50)* animals grown on the bacteria for RNAi against *tax-6* along with the EV control at 20°C. Day 0 represents young adults. p<0.001 (n = 3 biological replicates; animals per condition per replicate > 80).
(F) Representative photomicrographs of ORO stained 1-day-old adult *nhr-8(ok186)* animals grown on the EV control, *tax-6*, *flr-1*, *pbo-1*, and *nhx-2* RNAi bacteria at 20°C. Scale bar = 200 µm.
(G) Quantification of ORO intensity per animal of 1-day-old adult *nhr-8(ok186)* animals grown on the EV control, *tax-6*, *flr-1*, *pbo-1*, and *nhx-2* RNAi bacteria at 20°C. The values are area normalized for each animal. ***p<0.001 via the *t*-test (n = 20 worms each).
(H) Quantitative reverse transcription-PCR (qRT-PCR) for *nhr-8* mRNA levels in N2 animals grown on the EV control, *tax-6*, *flr-1*, *pbo-1*, and *nhx-2* RNAi bacteria at 20°C until 1-day-old adults. ***p < 0.001 via the *t*-test (n = 3 biological replicates).

reduced survival on *P. aeruginosa* following calcineurin inhibition is independent of HLH-30 and NHR-8 and is more likely due to increased gut colonization by *P. aeruginosa* resulting from DMP defects (**Figure 6C**).

Discussion

We discovered that calcineurin is required for the *C. elegans* DMP. Calcineurin activity is regulated by intracellular calcium levels. Increased amounts of calcium ions activate the phosphatase activity of calcineurin via the binding of the calcium-sensing protein calmodulin to calcineurin (Klee et al., 1998). The rhythmic DMP cycle in *C. elegans* is known to be regulated by rhythmic calcium waves (Santo et al., 1999; Teramoto and Iwasaki, 2006). The calcium waves are regulated by the endoplasmic reticulum calcium channel, ITR-1, and mutations in the *itr-1* gene affect defecation by preventing cytoplasmic calcium release (Santo et al., 1999). It is likely that calcium waves regulate DMP via calcineurin activities. Indeed, calcineurin is expressed in the enteric muscles that are required for contractions for DMP (Lee et al., 2005). It is interesting to note that *tax-6* gain-of-function mutants are also known to have DMP defects (Lee et al., 2005). Therefore, optimum calcineurin activity appears to be crucial for maintaining a rhythmic DMP.

Calcineurin inhibition has been shown to extend *C. elegans* lifespan via multiple mechanisms (Dong et al., 2007; Dwivedi et al., 2009; Mair et al., 2011; Tao et al., 2013). Activation of autophagy has been shown to be one of the mechanisms of extended lifespan upon calcineurin inhibition (Dwivedi et al., 2009). We showed that defects in the DMP caused by calcineurin inhibition reduce lipid levels and mimic calorie restriction. Calorie restriction is known to induce autophagy (Morselli et al., 2010), and autophagy is required for calorie restriction-mediated lifespan extension (Hansen et al., 2008; Jia and Levine, 2007). Therefore, it is likely that reduced lipid levels because of intestinal bloating result in the activation of autophagy upon calcineurin inhibition. Importantly, the TFEB ortholog, HLH-30, is required for lipolysis and autophagy under starvation conditions (Lapierre et al., 2013; O'Rourke and Ruvkun, 2013). HLH-30 is also required for lifespan enhancement via autophagy and multiple longevity pathways (Lapierre et al., 2013; O'Rourke and Ruvkun, 2013). We observed that HLH-30 is also required for the increase in lifespan upon calcineurin inhibition. Because autophagy may regulate lifespan via multiple longevity pathways (Hansen et al., 2008; Lapierre et al., 2013), this could explain why calcineurin inhibition enhances lifespan via multiple mechanisms.

Dietary restriction-mediated lifespan extensions are complex and context-dependent (Greer and Brunet, 2009). Multiple longevity pathways have been identified under different paradigms of dietary restriction (Chamoli et al., 2020, 2014; Chen et al., 2009; Greer and Brunet, 2009; Lapierre et al., 2013; Matai et al., 2019; Selman et al., 2009; Thondamal et al., 2014). We found that *tax-6* knockdown enhanced lifespan independent of multiple dietary restriction pathways, including *raga-1*, *rsks-1*, *daf-16*, and *nhr-49*. An earlier study identified that *tax-6* knockdown enhanced lifespan via NHR-49 (Burkewitz et al., 2015). We currently do not understand the reasons for this discrepancy. We identified that *tax-6* knockdown resulted in the upregulation of *nhr-8* mRNA levels, and *nhr-8* was required for the increased lifespan in *tax-6* knockdown animals. NHR-8 has been shown to mediate calorie restriction-dependent lifespan via the regulation of xenobiotic responses (Chamoli et al., 2014; Verma et al., 2018). It remains to be studied whether NHR-8 and HLH-30 work in the same or different pathways downstream of calcineurin inhibition (**Figure 6C**).

Recent studies in different organisms have shown that gut bloating has profound effects on food-seeking behaviors, immunity, and lifespan (Duvall et al., 2019; Filipowicz et al., 2021; Kumar et al., 2019; Min et al., 2021; Singh and Aballay, 2019a, 2019b, 2019c). Several *C. elegans* mutants with defects in the DMP and bloated intestinal lumens are known to have dampened nutrient absorption, leading to reduced lipid deposition in the gut, mimicking calorie restriction

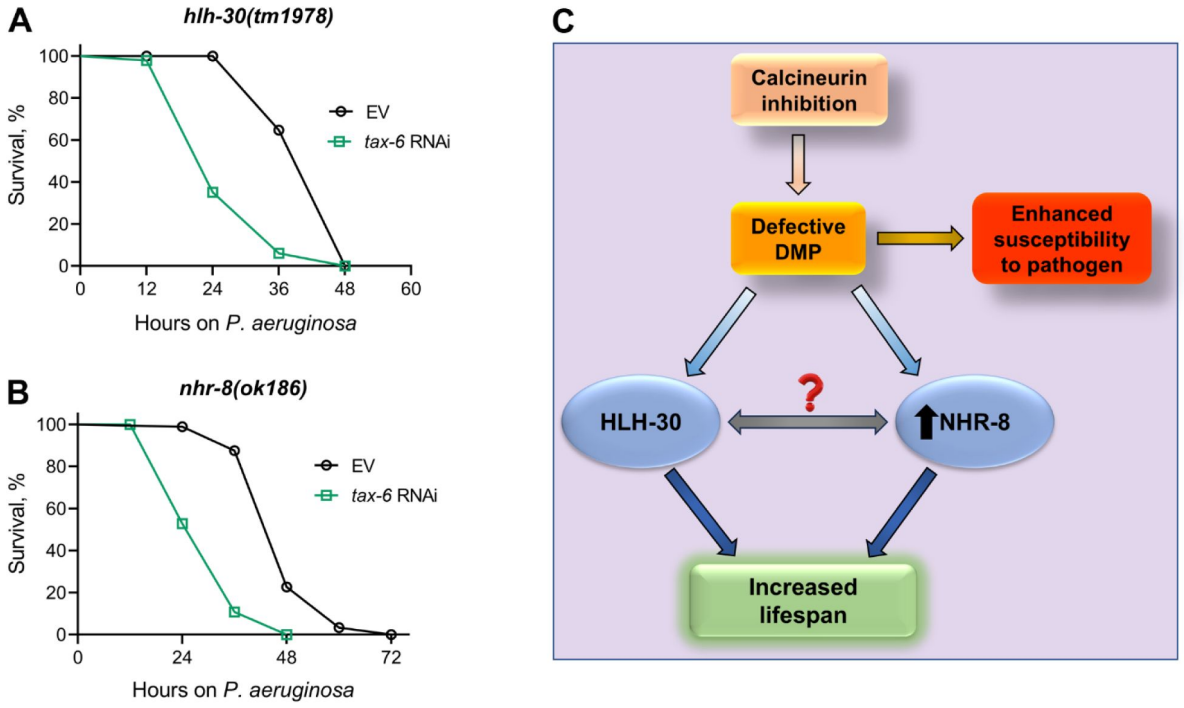

Figure 6

Calcineurin inhibition-mediated effects on lifespan and survival on *P. aeruginosa* are mediated by distinct mechanisms

(A)-(B) Representative survival plots of *hlh-30(tm1978)* (A) and *nhr-8(ok186)* (B) animals on *P. aeruginosa* PA14 at 25°C after treatment with the empty vector (EV) control and *tax-6* RNAi. $p<0.001$ for both the plots (n = 3 biological replicates; animals per condition per replicate > 85).
(C) Model depicting the mechanism of increased lifespan and enhanced susceptibility to pathogen upon inhibition of calcineurin via the defects in the defecation motor program (DMP).

(Sheng et al., 2015). It is possible that some of the effects of intestinal bloating on the host physiology are mediated by calorie restriction. Indeed, the neuropeptide Y receptors, which control a diverse set of behaviors, including appetite, are activated by gut bloating (Singh and Aballay, 2019c). Calorie restriction is known to induce neuropeptide Y, which might trigger feeding behaviors (Aveleira et al., 2015; de Rijke et al., 2005; Ferreira-Marques et al., 2016). The complete characterization of the physiological changes downstream of gut bloating may provide broad insights into the effects of gut physiology on behaviors, immunity, and lifespan.

Materials and methods

Key Resources Table				
Reagent type (species) or resource	**Designation**	**Source or reference**	**Identifiers**	**Additional information**
strain, strain background (*Escherichia coli*)	OP50	*Caenorhabditis* Genetics Center (CGC)	OP50	
strain, strain background (*E. coli*)	HT115(DE3)	Source BioScience	HT115(DE3)	
strain, strain background (*Pseudomonas aeruginosa*)	PA14	Frederick M Ausubel laboratory	PA14	
strain, strain background (*P. aeruginosa*)	PA14-GFP	Frederick M Ausubel laboratory	PA14-GFP	
strain, strain background (*Caenorhabditis elegans*)	N2 Bristol	CGC	N2	
strain, strain background (*C. elegans*)	*tax-6(p675)*	CGC	PR675	
strain, strain background (*C. elegans*)	*tax-6(ok2065)*	CGC	RB1667	
strain, strain background (*C. elegans*)	*fer-1(b232)*	CGC	HH142	
strain, strain background (*C. elegans*)	*eat-2(ad465)*	CGC	DA465	
strain, strain background (*C. elegans*)	*aak-2(ok524)*	CGC	RB754	

strain, strain background (*C. elegans*)	*raga-1(ok386)*	CGC	VC222	
strain, strain background (*C. elegans*)	*rsks-1(ok1255)*	CGC	RB1206	
strain, strain background (*C. elegans*)	*daf-16(mu86)*	CGC	CF1038	
strain, strain background (*C. elegans*)	*nhr-49(nr2041)*	CGC	STE68	
strain, strain background (*C. elegans*)	*hlh-30(tm1978)*	CGC	JIN1375	
strain, strain background (*C. elegans*)	*nhr-8(ok186)*	CGC	AE501	
strain, strain background (*C. elegans*)	*daf-9(rh50)*	CGC	RG1228	
strain, strain background (*C. elegans*)	*pmk-1(km25)*	CGC	KU25	
strain, strain background (*C. elegans*)	*kgb-1(km21)*	CGC	KU21	
strain, strain background (*C. elegans*)	*dbl-1(nk3)*	CGC	NU3	
strain, strain background (*C. elegans*)	*zip-2(ok3730)*	CGC	VC3056	
strain, strain background (*C. elegans*)	*clk-1(qm30)*	CGC	MQ130	

strain, strain background (*C. elegans*)	*isp-1(qm150)*	CGC	MQ887	
strain, strain background (*C. elegans*)	*sid-1(qt9)*	CGC	HC196	
strain, strain background (*C. elegans*)	*eat-2(ad465);tax-6(ok2065)*	This study		Materials and methods section
sequence-based reagent	Pan-act_qPCR_F	This study	qPCR primers	TCGGTATGGG ACAGAAGGAC
sequence-based reagent	Pan-act_qPCR_R	This study	qPCR primers	CATCCCAGTTG GTGACGATA
sequence-based reagent	pha-4_qPCR_F	This study	qPCR primers	CAAAGAGGAG CCAGAGTCGG
sequence-based reagent	pha-4_qPCR_R	This study	qPCR primers	TGTTTCTGCTC GCGTTTTCG
sequence-based reagent	nhr-8_qPCR_F	This study	qPCR primers	CTACACAGTTT CTCCGGCGT
sequence-based reagent	nhr-8_qPCR_R	This study	qPCR primers	GCCATTTGGG CCATAACACC
sequence-based reagent	tax-6(ok2065)_genotyping_F1	This study	Genotyping primers	CTCCTTTGAGG GAGCCAGTG
sequence-based reagent	tax-6(ok2065)_genotyping_F2	This study	Genotyping primers	CTGGGGACAA TCCACCATGAA
sequence-based reagent	tax-6(ok2065)_genotyping_R1	This study	Genotyping primers	TGTGTCCTGTA TCTGTGGGC

sequence-based reagent	eat-2(ad465)_genotyping_F	This study	Genotyping primers	CGGTGCAAAGAGCACATCTC
sequence-based reagent	eat-2(ad465)_genotyping_R	This study	Genotyping primers	TTAAGGCGTACGAGCCTTCC
software, algorithm	GraphPad Prism 8	GraphPad Software	RRID:SCR_002798	https://www.graphpad.com/scientificsoftware/prism/
software, algorithm	Photoshop CS5	Adobe	RRID:SCR_014199	https://www.adobe.com/products/photoshop.html
software, algorithm	ImageJ	NIH	RRID:SCR_003070	https://imagej.nih.gov/ij/

Bacterial strains

The following bacterial strains were used: *Escherichia coli* OP50, *E. coli* HT115(DE3), *Pseudomonas aeruginosa* PA14, and *P. aeruginosa* PA14 expressing green fluorescent protein (*P. aeruginosa* PA14-GFP). The cultures for these bacteria were grown in Luria-Bertani (LB) broth at 37°C.

C. elegans strains and growth conditions

C. elegans hermaphrodites were maintained on nematode growth medium (NGM) plates seeded with *E. coli* OP50 at 20°C unless otherwise indicated. Bristol N2 hermaphrodites were used as the wild-type control unless otherwise indicated. The strains used in the study are provided in the Key Resources Table. Some of the strains were obtained from the Caenorhabditis Genetics Center (University of Minnesota, Minneapolis, MN). The *eat-2(ad465);tax-6(ok2065)* strain was generated using a standard genetic cross. The *fer-1(b232)* hermaphrodites were maintained on *E. coli* OP50 at 15°C and were grown at 25°C prior to *P. aeruginosa* killing assays and longevity assays to obtain animals with unfertilized oocytes.

RNA interference (RNAi)

RNAi was used to generate loss-of-function phenotypes by feeding nematodes *E. coli* strain HT115(DE3) expressing double-stranded RNA homologous to a target gene. RNAi was carried out as described previously (Gokul and Singh, 2022; Ravi et al., 2023). Briefly, *E. coli* with the appropriate vectors were grown in LB broth containing ampicillin (100 µg/mL) at 37°C overnight and plated onto NGM plates containing 100 µg/mL ampicillin and 3 mM isopropyl β-D-thiogalactoside (IPTG) (RNAi plates). RNAi-expressing bacteria were allowed to grow overnight at 37°C. Gravid adults were transferred to RNAi-expressing bacterial lawns and allowed to lay eggs for 2 hours. The gravid adults were removed, and the eggs were allowed to develop at 20°C to 1-day-old adults for subsequent assays. The RNAi clones were from the Ahringer RNAi library and were verified by sequencing.

RNAi efficiency test

The RNAi efficiency test was carried out as described earlier (Gahlot and Singh, 2024; Ghosh and Singh, 2024). Briefly, the wild-type N2, *eat-2(ad456)*, *nhr-8(ok186)*, and *hlh-30(tm1978)* worms were synchronized by egg laying and grown on empty vector control, *act-5*, and *bli-3* RNAi plates

at 20°C. The *sid-1(qt9)* worms were used as RNAi-defective controls. After 72 hours, the animals were monitored for development defects and blisters on the cuticle for *act-5* and *bli-3* RNAi, respectively.

C. elegans longevity assays

Lifespan assays were performed on RNAi plates containing *E. coli* HT115(DE3) with the empty vector control and *tax-6* RNAi clone in the presence of 50 µg/mL of 5-fluorodeoxyuridine (FUdR). Animals were synchronized on RNAi plates without FUdR and incubated at 20°C. At the late L4 larval stage, the animals were transferred onto the corresponding RNAi plates containing 50 µg/mL of FUdR and incubated at 20°C. For *fer-1(b232)* lifespan assays, the animals were synchronized on RNAi plates without FUdR and incubated at 25°C. The *fer-1(b232)* lifespan assays were carried out at 25°C without FUdR. Animals were scored every other day as live, dead, or gone. Animals that failed to display touch-provoked movement were scored as dead. Animals that crawled off the plates were censored. Young adult animals were considered as day 0 for the lifespan analysis. Three independent experiments were performed.

C. elegans killing assays on P. aeruginosa PA14

Bacterial cultures were prepared by inoculating individual bacterial colonies of *P. aeruginosa* into 2 mL of LB and growing them for 10-12 hours on a shaker at 37°C. Bacterial lawns were prepared by spreading 20 µL of the culture on the entire surface of 3.5-cm-diameter modified NGM agar plates (0.35% instead of 0.25% peptone). The plates were incubated at 37°C for 12-16 hours and then cooled to room temperature for at least 30 minutes before seeding with synchronized 1-day-old adult animals. The killing assays were performed at 25°C, and live animals were transferred daily to fresh plates. Animals were scored at times indicated and were considered dead when they failed to respond to touch.

P. aeruginosa-GFP colonization assay

Bacterial cultures were prepared by inoculating individual bacterial colonies of *P. aeruginosa*-GFP into 2 mL of LB and growing them for 10-12 hours on a shaker at 37°C. Bacterial lawns were prepared by spreading 20 µL of the culture on the entire surface of 3.5-cm-diameter modified NGM agar plates (0.35% instead of 0.25% peptone) containing 50 µg/mL of kanamycin. The plates were incubated at 37°C for 12 hours and then cooled to room temperature for at least 30 minutes before seeding with 1-day-old adult gravid adults. The assays were performed at 25°C. After 6 hours of incubation, the animals were transferred from *P. aeruginosa*-GFP plates to fresh *E. coli* OP50 plates and visualized within 5 minutes under a fluorescence microscope.

Quantification of intestinal bacterial loads

The intestinal bacterial loads were quantified by measuring colony-forming units (CFU) as described earlier (Singh and Aballay, 2019b, 2019a) with appropriate modifications. Briefly, *P. aeruginosa*-GFP lawns were prepared as described above. After 6 hours of exposure, the animals were transferred from *P. aeruginosa*-GFP plates to the center of fresh *E. coli* OP50 plates thrice for 10 minutes each to eliminate bacteria stuck to their body. Afterward, ten animals/condition were transferred into 50 µL of PBS containing 0.01% triton X-100 and ground using glass beads. Serial dilutions of the lysates (10^1, 10^2, 10^3, 10^4) were seeded onto LB plates containing 50 µg/mL of kanamycin to select for *P. aeruginosa*-GFP cells and grown overnight at 37°C. Single colonies were counted the next day and represented as the number of bacterial cells or CFU per animal. At least three independent experiments were performed for each condition.

Fluorescence imaging

Fluorescence imaging was carried out as described previously (Gokul and Singh, 2022; Ravi et al., 2023). Briefly, the animals were anesthetized using an M9 salt solution containing 50 mM sodium azide and mounted onto 2% agarose pads. The animals were then visualized using a Nikon SMZ-1000 fluorescence stereomicroscope.

Quantification of intestinal lumen bloating

The 1-day-old adult animals grown on the empty vector control and *tax-6* RNAi were anesthetized using an M9 salt solution containing 50 mM sodium azide, mounted onto 2% agarose pads, and imaged. The diameter of the intestinal lumen was measured using the Zeiss Zen Pro 2011 software. At least ten animals were used for each condition.

Measurement of defecation motor program (DMP) rate

Wild-type N2 and *tax-6(p675)* animals were synchronized and grown at 20°C on *E. coli* OP50 for 4 and 5 days, respectively, before measuring the DMP rate. For RNAi experiments, N2 worms were synchronized on EV and *tax-6* RNAi plates and grown for 4 days at 20°C before measuring the DMP rate. The DMP cycle length was scored by assessing the time between expulsions (which are preceded by posterior and anterior body wall muscle contraction and the contraction of enteric muscles in a normal regular pattern) (Thomas, 1990). The number of expulsion events in 20 minutes was measured for each worm. The DMP rate was recorded for 5-6 worms/condition.

Ethogram for DMP

Wild type N2 and *tax-6(ok2065)* worms were synchronized by egg laying and grown at 20°C on *E. coli* OP50 for 4 and 5 days, respectively. For RNAi experiments, N2 worms were synchronized and grown on empty vector control and *tax-6* RNAi at 20°C for 4 days. The assay was performed at 25°C. The defecation motor program consists of three steps-posterior body-wall muscle contraction (p), anterior body-wall muscle contraction (a), and expulsion muscle contraction (x). Animals were observed for the exact time of these three contractions on a dissecting scope for a continuous period of 20 minutes. A computer program was developed to plot the ethogram where we manually input the timings of “p”, “a”, and “x” contractions.

Blue dye assay to assess functional defecation rate

Wild type N2 and *tax-6(ok2065)* worms were synchronized by egg laying and grown at 20°C on *E. coli* OP50 for 4 and 5 days, respectively, before measuring the functional defecation rate. For RNAi experiments, N2 worms were synchronized and grown on empty vector control and *tax-6* RNAi at 20°C for 4 days. The functional defecation rate was assessed using a blue dye, erioglaucine disodium salt (5% wt/v), as an indicator of gut content. The time required by worms to clear the blue dye from the gut was used to calculate a functional defecation rate. Briefly, 50 worms from each condition were incubated in a solution containing blue dye and *E. coli* OP50 culture in a 1:1 ratio for 2 hours. Then, the worms were transferred to an NGM plate seeded with *E. coli* OP50. About 25-27 worms from each condition were transferred to a fresh NGM plate seeded with *E. coli* OP50. The functional defecation rate was assessed by observing the clearance of blue dye from the intestine of worms every 5 minutes over a period of 60 minutes. Three independent experiments were performed for each condition.

Pharyngeal pumping assay

For the pharyngeal pumping assay, 1-day-old adult animals grown on the empty vector control and *tax-6* RNAi were used. The number of contractions of the terminal bulb of the pharynx was counted for 30 seconds per worm. The pumping rates for 20 worms were recorded for each condition.

Lipid staining

The oil-red-O (ORO) staining was carried out as described earlier (Lynn et al., 2015) with appropriate modification. Briefly, wild-type N2, *hlh-30(tm1978)*, and *nhr-8(ok186)* animals were synchronized on empty vector control and *tax-6* RNAi bacteria and grown at 20°C for 4 days. About 300-400 synchronized gravid adult worms from experimental plates were washed three times with 1X PBS plus 0.01% triton X-100 (PBST). To permeabilize the cuticle, 600 µL of 40% isopropanol was added to 100 µL of worm pellet and was rocked for three minutes. The animals were spun down at 500 rpm for 30 seconds, and then 600 µL of supernatant was removed. Subsequently, 600 µL of ORO working stock was added to the worm pellet to stain the worms and incubated at room temperature for 1 hour on a shaker. ORO working stock was freshly prepared by diluting the stock 0.5% ORO in isopropanol to 60% in water and rocked at room temperature for 2 hours, followed by the removal of debris with a 0.22 µm filter. Afterward, worm samples were pelleted, 600 µL of supernatant was removed, 600 µL of PBST was added, and the samples were rocked for 30 minutes at room temperature. After that, the worms were mounted on a 2% agarose pad and imaged. At least ten worms/condition were imaged. Three independent biological replicates were performed. The ORO intensity was quantified using Image J software.

RNA isolation and quantitative reverse transcription-PCR (qRT-PCR)

Animals were synchronized by egg laying. Approximately 40 N2 gravid adult animals were transferred to 9-cm RNAi plates seeded with *E. coli* HT115 expressing the appropriate vectors and allowed to lay eggs for 4-5 hours. The gravid adults were then removed, and the eggs were allowed to develop at 20°C for 96 hours. Subsequently, the animals were collected, washed with M9 buffer, and frozen in TRIzol reagent (Life Technologies, Carlsbad, CA). Total RNA was extracted using the RNeasy Plus Universal Kit (Qiagen, Netherlands). Residual genomic DNA was removed using TURBO DNase (Life Technologies, Carlsbad, CA). A total of 6 µg of total RNA was reverse-transcribed with random primers using the High-Capacity cDNA Reverse Transcription Kit (Applied Biosystems, Foster City, CA).

qRT-PCR was conducted using the Applied Biosystems One-Step Real-time PCR protocol using SYBR Green fluorescence (Applied Biosystems) on an Applied Biosystems 7900HT real-time PCR machine in 96-well-plate format. Twenty-five-microliter reactions were analyzed as outlined by the manufacturer (Applied Biosystems). The relative fold-changes of the transcripts were calculated using the comparative *CT*($2^{-\Delta\Delta CT}$) method and normalized to pan-actin (*act-1, -3, -4*) as described earlier (Singh and Aballay, 2019a, 2017). The cycle thresholds of the amplification were determined using StepOnePlus software (Applied Biosystems). All samples were run in triplicate. The primer sequences are provided in the Key Resources Table.

Quantification and statistical analysis

The statistical analysis was performed with Prism 8 (GraphPad). All error bars represent mean±standard deviation (SD). The unpaired, two-tailed, two-sample *t*-test was used when needed, and the data were judged to be statistically significant when $p < 0.05$. In the figures, asterisks (*) denote statistical significance as follows: *, $p<0.05$, **, $p<0.01$, ***, $p<0.001$, as compared with the appropriate controls. The Kaplan-Meier method was used to calculate the survival fractions, and statistical significance between survival curves was determined using the log-rank test. All experiments were performed in triplicate.

Acknowledgements

We thank Sagar Santosh Gawande for help in plotting the DMP ethogram. Some strains used in this study were provided by the Caenorhabditis Genetics Center (CGC), which is funded by the NIH Office of Research Infrastructure Programs (P40 OD010440).

Funding

This work was supported by the following grants: Har-Gobind Khorana-Innovative Young Biotechnologist Fellowship (File No. HRD-17011/2/2023-HRD-DBT) and Ramalingaswami Re-entry Fellowship (Ref. No. BT/RLF/Re-entry/50/2020) awarded by the Department of Biotechnology, India; STARS grant (File No. MoE-STARS/STARS-2/2023-0116) awarded by the Ministry of Education, India; Research Grant (Ref. No. 37/1741/23/EMR-II) awarded by the Council of Scientific & Industrial Research (CSIR), India; Science and Engineering Research Board (SERB) Startup Research Grant (Ref. No. SRG/2020/000022) and Core Research Grant (Ref. No. CRG/2023/001136) awarded by DST, India; and IISER Mohali intramural funds. P.D. was supported by a senior research fellowship from the Council of Scientific & Industrial Research (CSIR), India.

Author contributions

Priyanka Das: Conceptualization, Data curation, Formal analysis, Investigation, Methodology

Alejandro Aballay: Conceptualization, Visualization, Supervision

Jogender Singh: Conceptualization, Data curation, Formal analysis, Funding acquisition, Investigation, Methodology, Project administration, Visualization, Supervision, Writing— original draft, Writing – review and editing

Competing interest: The authors declare that they have no competing interest.

Supplementary figures

Figure S1

Calcineurin knockdown enhances *C. elegans* susceptibility to *P. aeruginosa*

Representative survival plots of N2 animals on *P. aeruginosa* PA14 at 25°C after treatment with the empty vector (EV) control, *tax-6*, *crtc-1*, and *crh-1* RNAi. . p<0.001 for *tax-6* and p<0.01 for *crtc-1* and *crh-1* compared to EV (n = 3 biological replicates; animals per condition per replicate > 85).

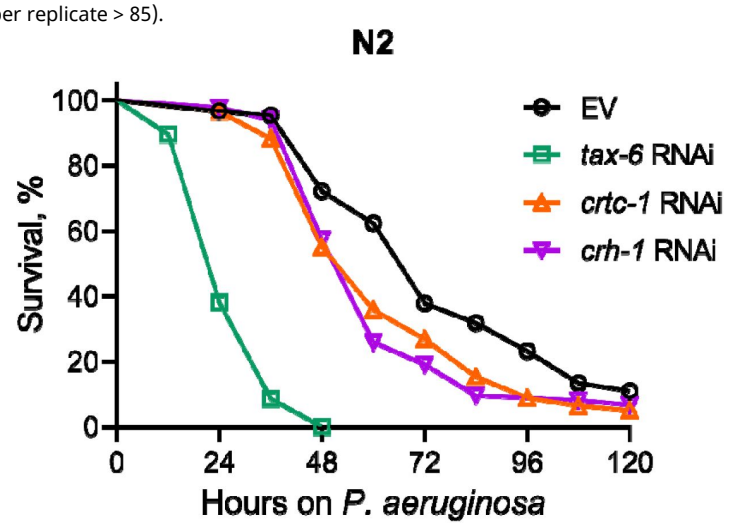

Figure S2

Calcineurin inhibition enhances susceptibility to *P. aeruginosa* independent of known immunity pathways

(A-E) Representative survival plots of *pmk-1(km25)* (A), *kgb-1(km21)* (B), *dbl-1(nk3)* (C), *zip-2(ok3730)* (D), and *daf-16(mu86)* (E) animals on *P. aeruginosa* PA14 at 25°C after treatment with the empty vector (EV) control and *tax-6* RNAi. p<0.001 for all the plots (n = 3 biological replicates; animals per condition per replicate > 90).

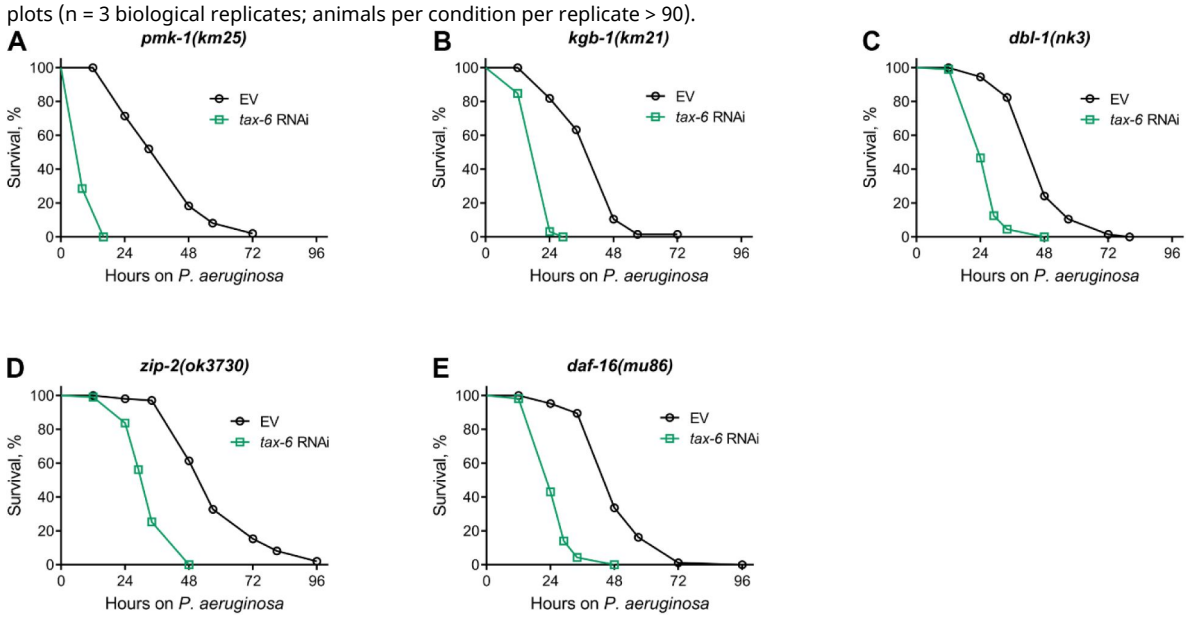

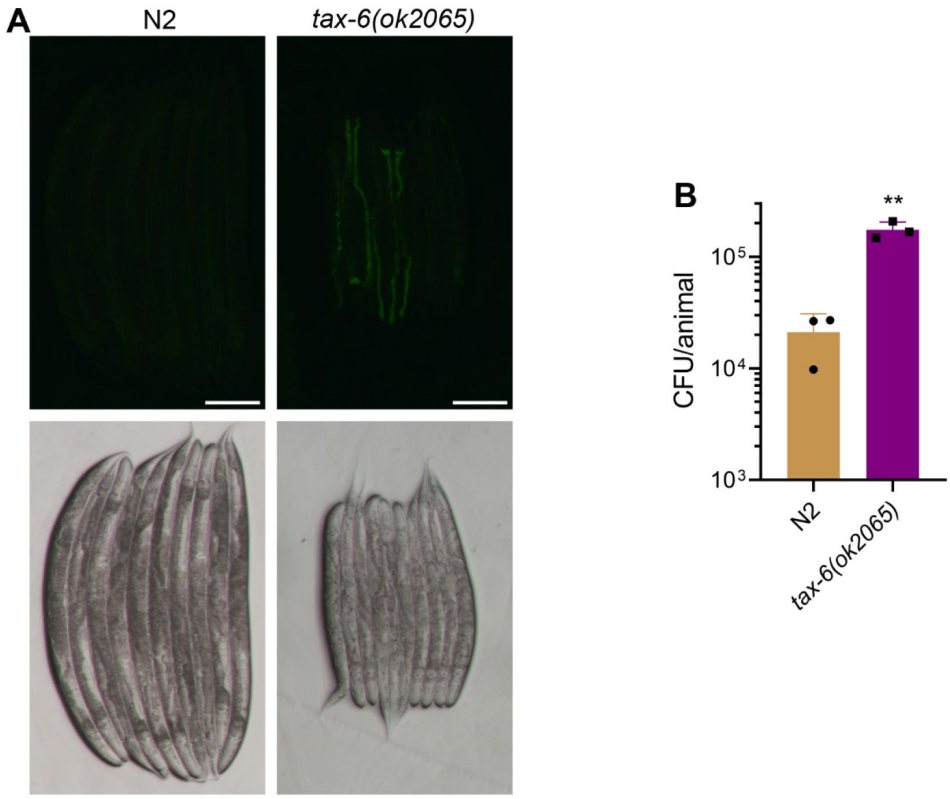

Figure S3

Calcineurin is required for the *C. elegans* defecation motor program (DMP)

(A) Representative fluorescence (top) and the corresponding brightfield (bottom) images of N2 and *tax-6(ok2065)* animals incubated on *P. aeruginosa*-GFP for 6 hours at 25°C after growth on *E. coli* OP50 at 20°C. Scale bar = 200 µm.
(B) CFU per animal of N2 and *tax-6(ok2065)* worms incubated on *P. aeruginosa*-GFP for 6 hours at 25°C after growth on *E. coli* OP50 at 20°C. **p < 0.01 via the *t*-test (n = 3 biological replicates).

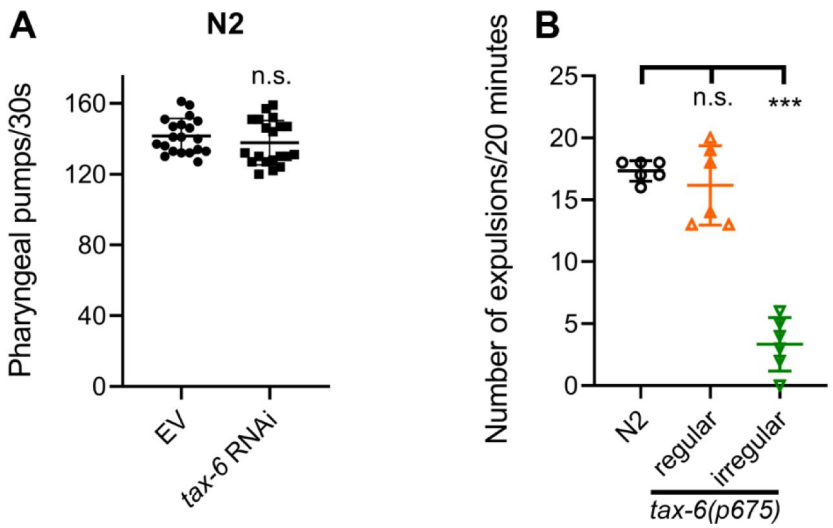

Figure S4

Calcineurin inhibition leads to defects in the defecation motor program (DMP) without affecting the pharyngeal pumping rate

(A) Pharyngeal pumps per 30 seconds of 1-day-old adult N2 animals grown on the empty vector (EV) control and *tax-6* RNAi bacteria at 20°C. n.s., nonsignificant via the *t*-test (n = 20 worms each).
(B) The number of expulsion events observed in 20 minutes in 1-day-old adult N2 and regular and irregular *tax-6(p675)* animals grown on *E. coli* OP50 at 20°C. ***p<0.001, n.s., nonsignificant via the *t*-test (n = 6 worms each).

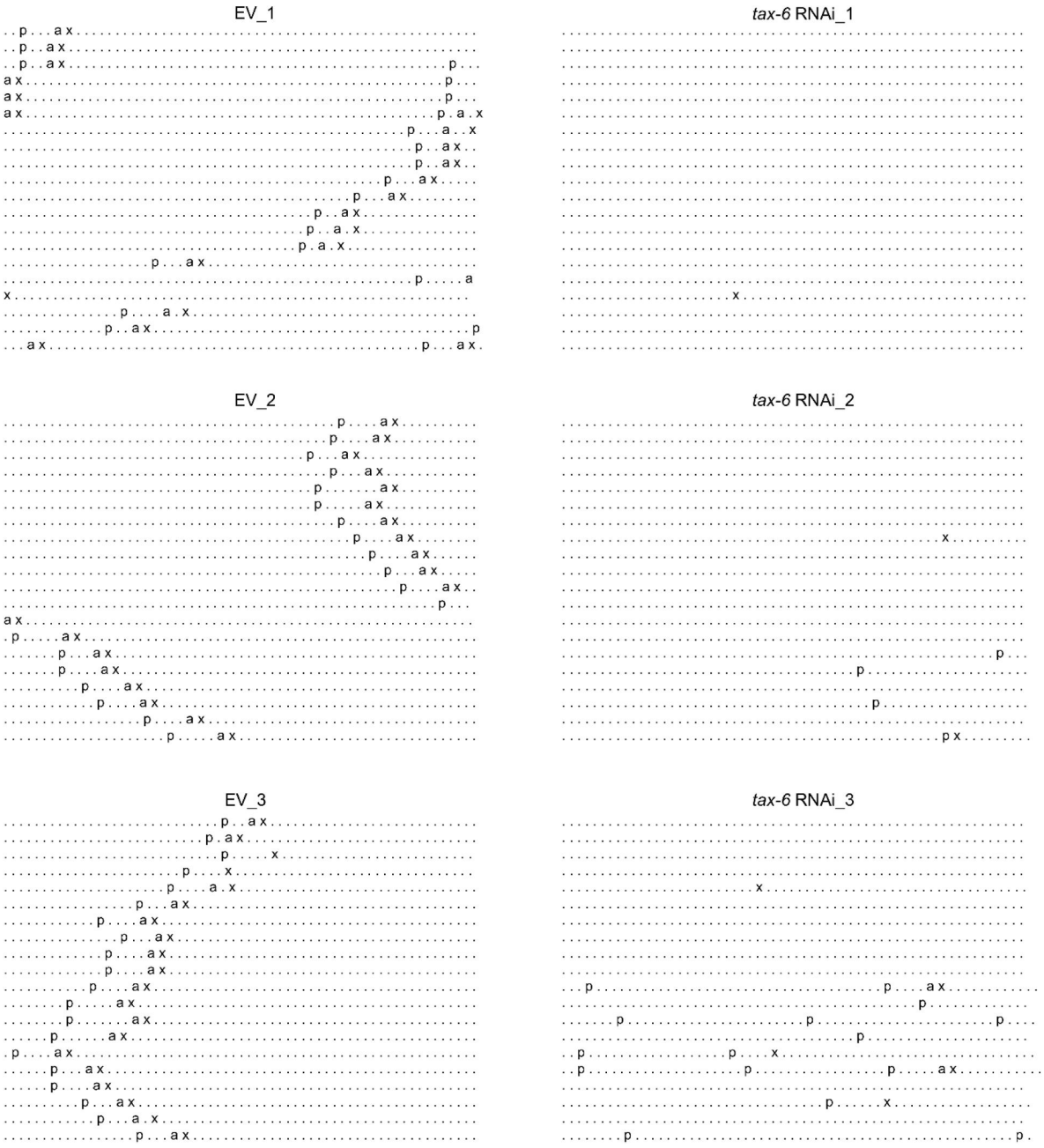

Figure S5

Calcineurin inhibition disrupts the *C. elegans* defecation motor program (DMP)

Three different DMP ethograms of N2 animals after growth on each empty vector (EV) control and *tax-6* RNAi bacteria till 1-day-old stage. Each dot represents a second, and each row represents a minute. 'p', 'a', and 'x' represent posterior body-wall muscle contraction, anterior body-wall muscle contraction, and expulsion muscle contraction, respectively.

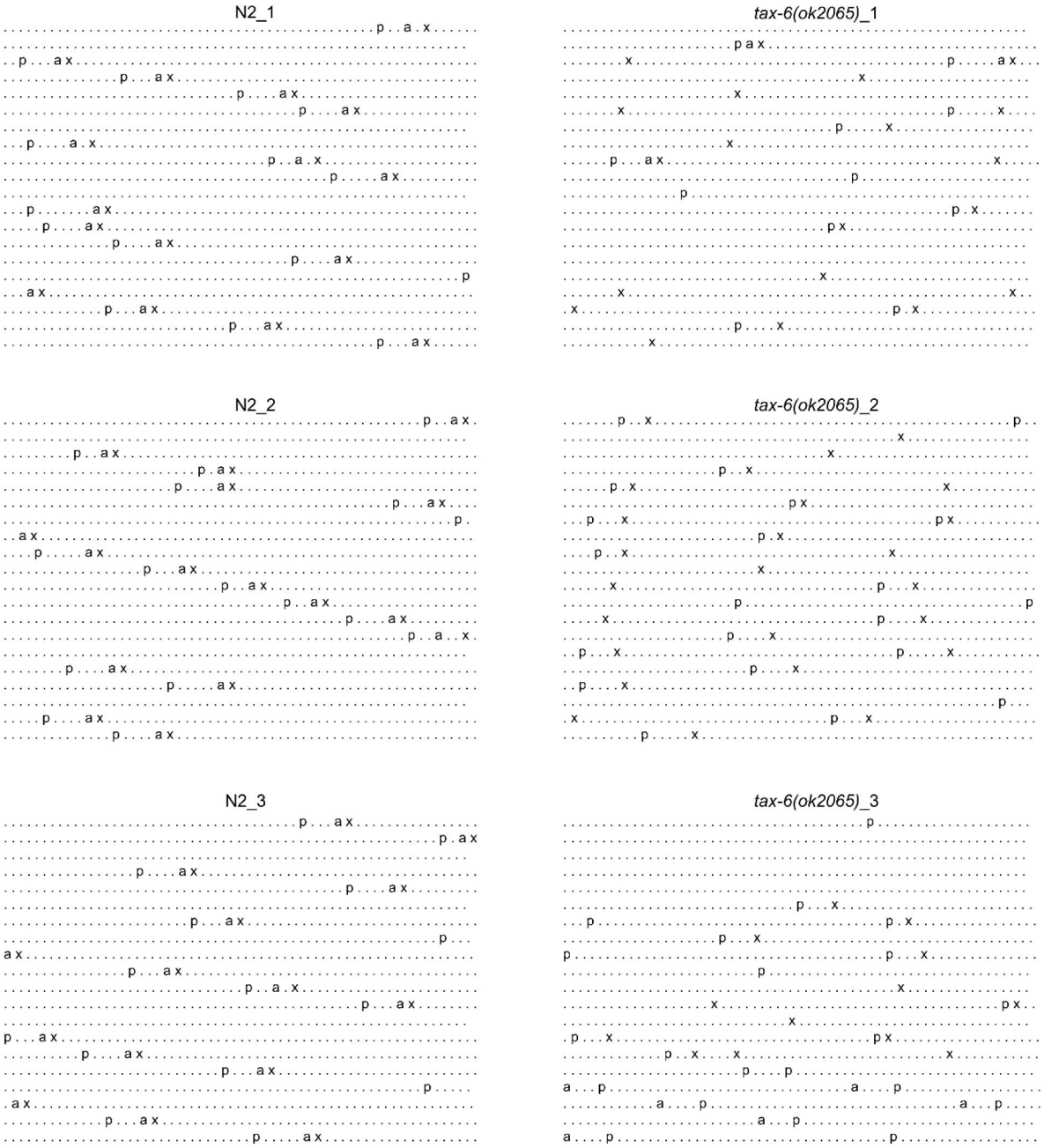

Figure S6

Calcineurin inhibition disrupts the *C. elegans* defecation motor program (DMP)

Three different DMP ethograms of N2 and *tax-6(ok2065)* animals each after their growth on *E. coli* OP50 at 20°C till the 1-day-old adult stage. Each dot represents a second, and each row represents a minute. 'p', 'a', and 'x' represent posterior body-wall muscle contraction, anterior body-wall muscle contraction, and expulsion muscle contraction, respectively.

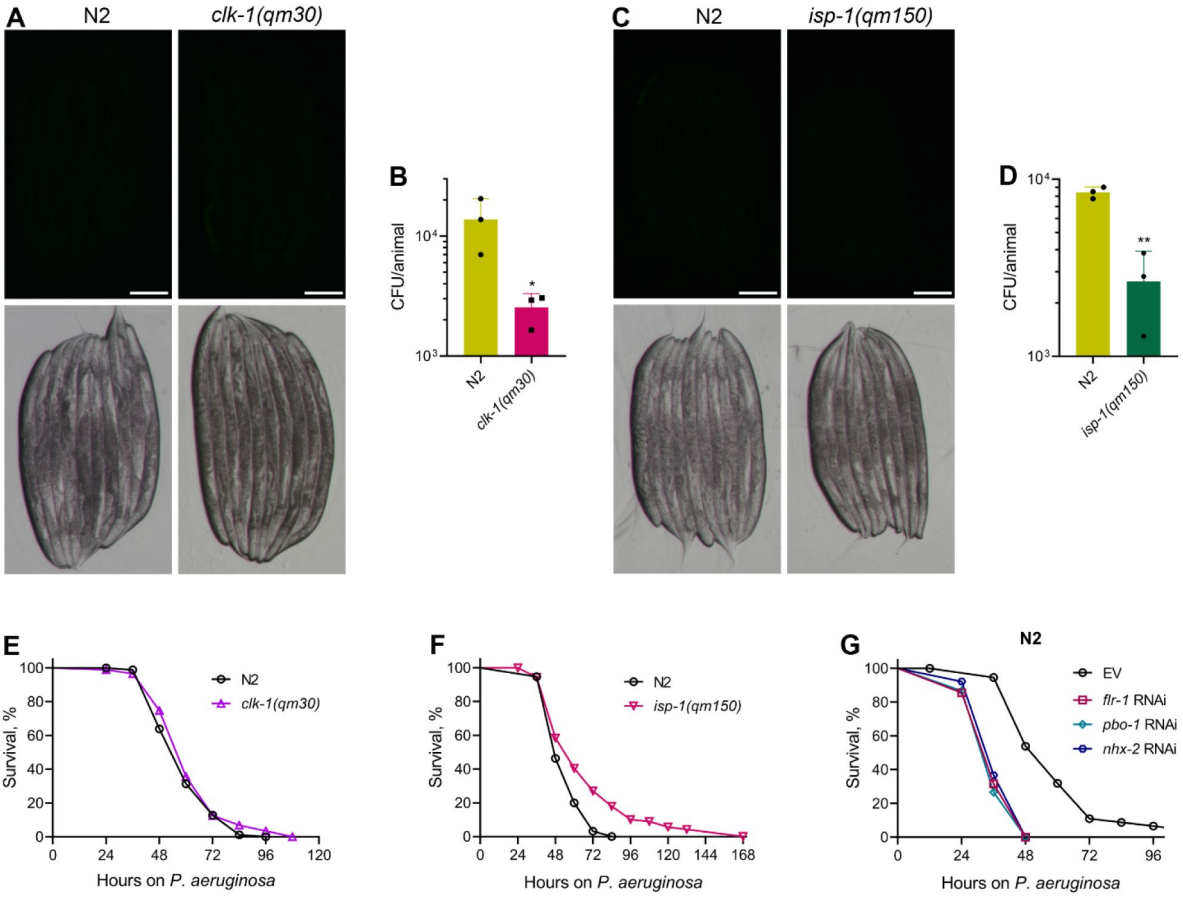

Figure S7

Slow DMP versus disrupted DMP lead to distinct phenotypes on *P. aeruginosa* exposure

(A) Representative fluorescence (top) and the corresponding brightfield (bottom) images of N2 and *clk-1(qm30)* animals incubated on *P. aeruginosa*-GFP for 6 hours at 25°C after growth on *E. coli* OP50 at 20°C. Scale bar = 200 µm.
(B) CFU per animal of N2 and *clk-1(qm30)* worms incubated on *P. aeruginosa*-GFP for 6 hours at 25°C after growth on *E. coli* OP50 at 20°C. *p < 0.05 via the *t*-test (n = 3 biological replicates).
(C) Representative fluorescence (top) and the corresponding brightfield (bottom) images of N2 and *isp-1(qm150)* animals incubated on *P. aeruginosa*-GFP for 6 hours at 25°C after growth on *E. coli* OP50 at 20°C. Scale bar = 200 µm.
(D) CFU per animal of N2 and *isp-1(qm150)* worms incubated on *P. aeruginosa*-GFP for 6 hours at 25°C after growth on *E. coli* OP50 at 20°C. **p < 0.01 via the *t*-test (n = 3 biological replicates).
(E) Representative survival plots of N2 and *clk-1(qm30)* animals on *P. aeruginosa* PA14 at 25°C. The animals were grown on *E. coli* OP50 at 20°C until 1-day-old adults before transferring to *P. aeruginosa* PA14 at 25°C. n.s., nonsignificant (n = 3 biological replicates; animals per condition per replicate > 90).
(F) Representative survival plots of N2 and *isp-1(qm150)* animals on *P. aeruginosa* PA14 at 25°C. The animals were grown on *E. coli* OP50 at 20°C until 1-day-old adults before transferring to *P. aeruginosa* PA14 at 25°C. p<0.001 (n = 3 biological replicates; animals per condition per replicate > 90).
(G) Representative survival plots of N2 animals on *P. aeruginosa* PA14 at 25°C after treatment with the empty vector (EV) control, *flr-1*, *pbo-1*, and *nhx-2* RNAi. p<0.001 for *flr-1*, *pbo-1*, and *nhx-2* RNAi compared to EV (n = 3 biological replicates; animals per condition per replicate > 90).

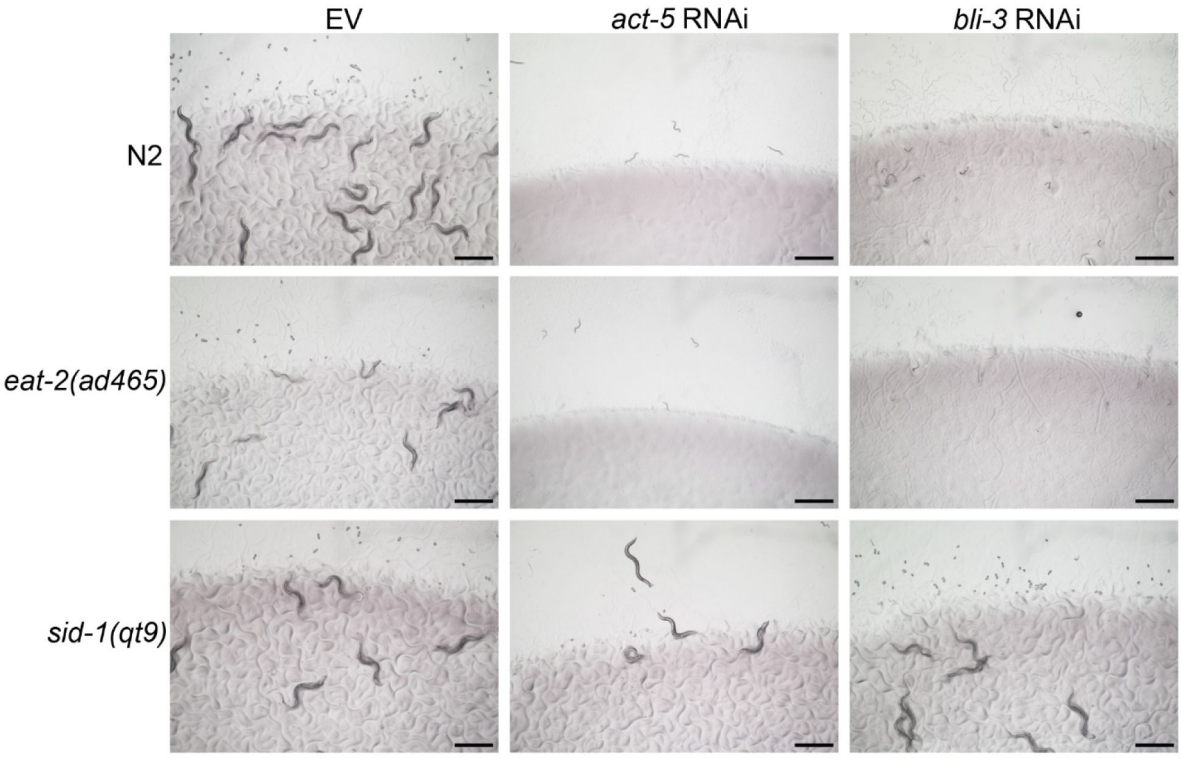

Figure S8

The *eat-2(ad465)* animals are not defective in RNAi

Representative images of wild-type N2, *eat-2(ad465)*, and *sid-1(qt9)* worms on the empty vector (EV) control, *act-5*, and *bli-3* RNAi. Scale bar = 1 mm.

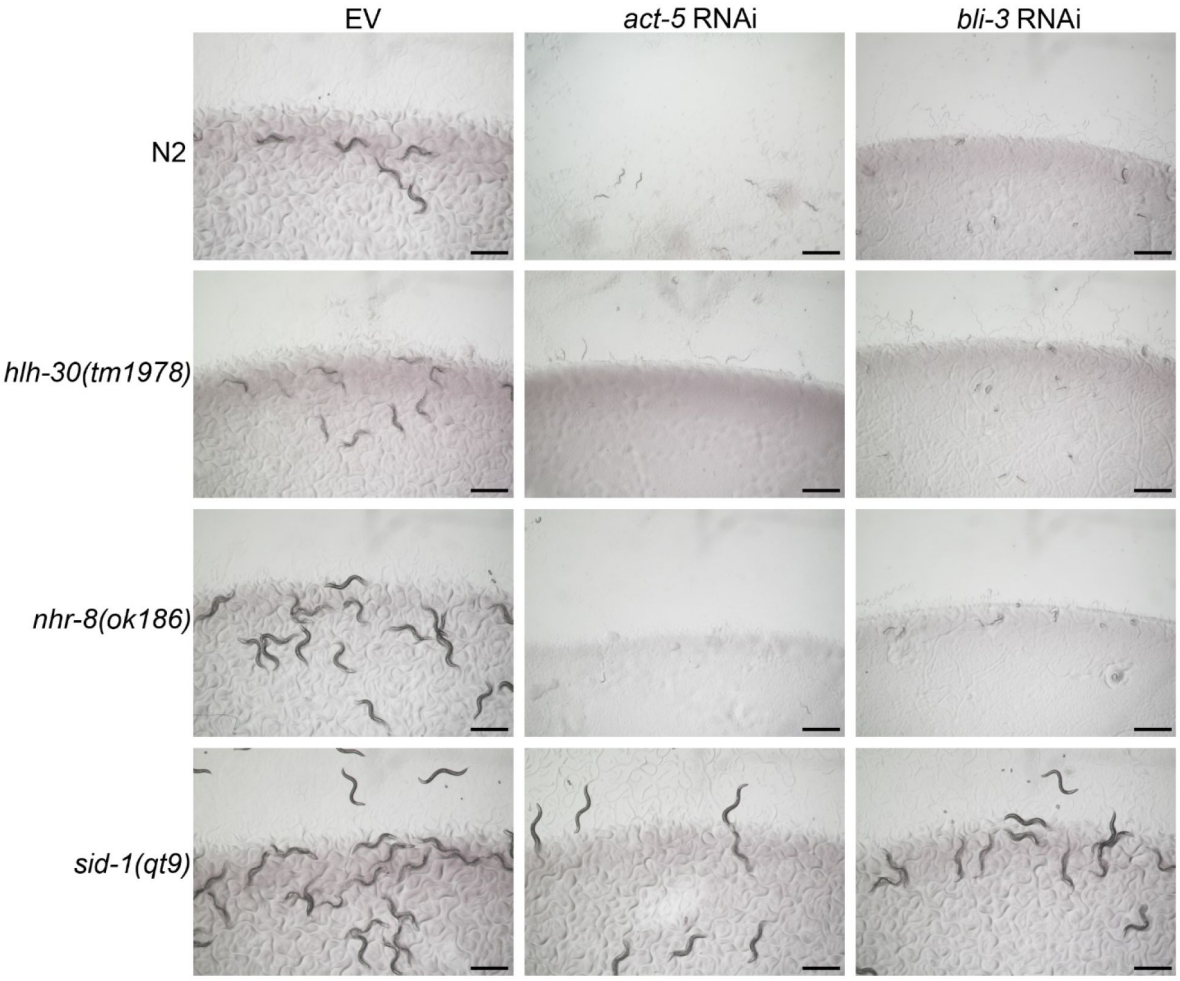

Figure S9

The *hlh-30(tm1978)* and *nhr-8(ok186)* animals are not defective in RNAi

Representative images of wild-type N2, *hlh-30(tm1978)*, *nhr-8(ok186)*, and *sid-1(qt9)* worms on the empty vector (EV) control, *act-5*, and *bli-3* RNAi. Scale bar = 1 mm.

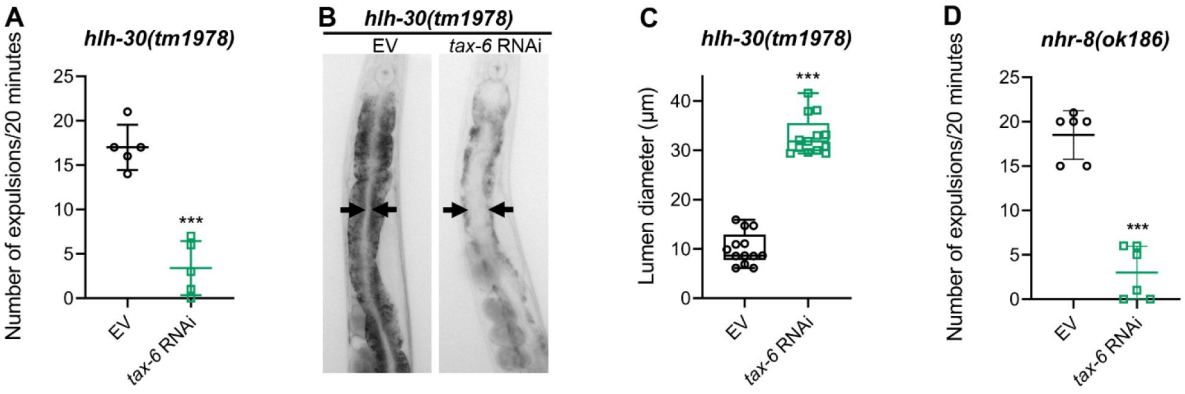

Figure S10

Calcineurin inhibition leads to defects in the defecation motor program (DMP) in *hlh-30(tm1978)* and *nhr-8(ok186)* animals

(A) The number of expulsion events observed in 20 minutes in 1-day-old adult *hlh-30(tm1978)* animals grown on the empty vector (EV) control and *tax-6* RNAi bacteria at 20°C. ***p<0.001 via the *t*-test (n = 5 worms each).
(B) Representative photomicrographs of *hlh-30(tm1978)* animals grown on the EV control and *tax-6* RNAi bacteria at 20°C until 1-day-old adults. Arrows point to the border of the intestinal lumen.
(C) Quantification of the diameter of the intestinal lumen of *hlh-30(tm1978)* animals grown on the EV control and *tax-6* RNAi bacteria at 20°C until 1-day-old adults. ***p<0.001 via the *t*-test (n = 13 worms each).
(D) The number of expulsion events observed in 20 minutes in 1-day-old adult *nhr-8(ok186)* animals grown on the EV control and *tax-6* RNAi bacteria at 20°C. ***p<0.001 via the *t*-test (n = 6 worms each).

References

1. Alper S, Mcelwee MK, Apfeld J, Lackford B, Freedman JH, Schwartz DA (2010) **The Caenorhabditis elegans Germ Line Regulates Distinct Signaling Pathways to Control Lifespan and Innate Immunity** *J Biol Chem* **285**:1822–1828 https://doi.org/10.1074/jbc.M109.057323

2. Amrit FRG *et al.* (2019) **The longevity-promoting factor, TCER-1, widely represses stress resistance and innate immunity** *Nat Commun* **10** https://doi.org/10.1038/s41467-019-10759-z

3. Argon Y, Ward S (1980) **Caenorhabditis elegans fertilization-defective mutants with abnormal sperm** *Genetics* **96**:413–433

4. Aveleira CA *et al.* (2015) **Neuropeptide Y stimulates autophagy in hypothalamic neurons** *Proc Natl Acad Sci U S A* **112**:E1642–E1651 https://doi.org/10.1073/pnas.1416609112

5. Bandyopadhyay J *et al.* (2002) **Calcineurin, a Calcium / Calmodulin-dependent Protein Phosphatase, Is Involved in Movement, Fertility, Egg Laying, and Growth in Caenorhabditis elegans** *Mol Biol Cell* **13**:3281–3293 https://doi.org/10.1091/mbc.E02

6. Burkewitz K, Morantte I, Weir HJM, Yeo R, Zhang Y, Huynh FK, Ilkayeva OR, Hirschey MD, Grant AR, Mair WB (2015) **Neuronal CRTC-1 Governs Systemic Mitochondrial Metabolism and Lifespan via a Catecholamine Signal** *Cell* **160**:842–855 https://doi.org/10.1016/j.cell.2015.02.004

7. Campos JC, Wu Z, Rudich PD, Soo SK, Mistry M, Ferreira JCB, Blackwell TK, Van Raamsdonk JM (2021) **Mild mitochondrial impairment enhances innate immunity and longevity through ATFS-1 and p 38 signaling** *EMBO Rep* **22** https://doi.org/10.15252/embr.202152964

8. Castro E de, Castro SH de, Johnson TE (2004) **Isolation of long-lived mutants in Caenorhabditis elegans using selection for resistance to juglone** *Free Radic Biol Med* **37**:139–145 https://doi.org/10.1016/j.freeradbiomed.2004.04.021

9. Chamoli M, Goyala A, Tabrez SS, Siddiqui AA, Singh A, Antebi A, Lithgow GJ, Watts JL, Mukhopadhyay A (2020) **Polyunsaturated fatty acids and p38-MAPK link metabolic reprogramming to cytoprotective gene expression during dietary restriction** *Nat Commun* **11** https://doi.org/10.1038/s41467-020-18690-4

10. Chamoli M, Singh A, Malik Y, Mukhopadhyay A (2014) **A novel kinase regulates dietary restriction-mediated longevity in Caenorhabditis elegans** *Aging Cell* **13**:641–655 https://doi.org/10.1111/acel.12218

11. Chen D, Thomas EL, Kapahi P (2009) **HIF-1 Modulates Dietary Restriction-Mediated Lifespan Extension via IRE-1 in Caenorhabditis elegans** *PLoS Genet* **5** https://doi.org/10.1371/journal.pgen.1000486

12. Chen L, Song M, Yao C (2022) **Calcineurin in development and disease** *Genes Dis* **9**:915–927 https://doi.org/10.1016/j.gendis.2021.03.002

13. de Rijke CE, Hillebrand JJG, Verhagen LAW, Roeling TAP, Adan RAH (2005) **Hypothalamic neuropeptide expression following chronic food restriction in sedentary and wheel-running rats** *J Mol Endocrinol* **35**:381–390 https://doi.org/10.1677/jme.1.01808

14. Denzel MS, Storm NJ, Gutschmidt A, Baddi R, Hinze Y, Jarosch E, Sommer T, Hoppe T, Antebi A (2014) **Hexosamine pathway metabolites enhance protein quality control and prolong life** *Cell* **156**:1167–1178 https://doi.org/10.1016/j.cell.2014.01.061

15. Dong M-Q, Venable JD, Au N, Xu T, Park SK, Cociorva D, Johnson JR, Dillin A, Yates JR (2007) **Quantitative Mass Spectrometry Identifies Insulin Signaling Targets in C. elegans** *Science* **80**:660–663 https://doi.org/10.1126/science.1139952

16. Duvall LB, Ramos-Espiritu L, Barsoum KE, Glickman JF, Vosshall LB (2019) **Small-Molecule Agonists of Ae. aegypti Neuropeptide Y Receptor Block Mosquito Biting** *Cell* **176**:687–701 https://doi.org/10.1016/j.cell.2018.12.004

17. Dwivedi M, Song HO, Ahnn J (2009) **Autophagy genes mediate the effect of calcineurin on life span in C. elegans** *Autophagy* **5**:604–607 https://doi.org/10.4161/auto.5.5.8157

18. Estes KA, Dunbar TL, Powell JR, Ausubel FM, Troemel ER (2010) **bZIP transcription factor zip-2 mediates an early response to Pseudomonas aeruginosa infection in Caenorhabditis elegans** *Proc Natl Acad Sci* **107**:2153–2158 https://doi.org/10.1073/pnas.0914643107

19. Fabian DK, Fuentealba M, Melike H, Partridge L, Thornton JM (2021) **Functional conservation in genes and pathways linking ageing and immunity** *Immun Ageing* **18**

20. Feng J, Bussière F, Hekimi S (2001) **Mitochondrial Electron Transport Is a Key Determinant of Life Span in Caenorhabditis elegans** *Dev Cell* **1**:633–644 https://doi.org/10.1016/S1534-5807(01)00071-5

21. Ferreira-Marques M, Aveleira CA, Carmo-Silva S, Botelho M, de Almeida LP, Cavadas C (2016) **Caloric restriction stimulates autophagy in rat cortical neurons through neuropeptide Y and ghrelin receptors activation** *Aging (Albany NY* **8**:1470–1484 https://doi.org/10.18632/aging.100996

22. Filipowicz A, Lalsiamthara J, Aballay A (2021) **Trpm channels mediate learned pathogen avoidance following intestinal distention** *Elife* **10** https://doi.org/10.7554/eLife.65935

23. Gahlot S, Singh J (2024) **Caenorhabditis elegans neuronal RNAi does not render other tissues refractory to RNAi** *Proc Natl Acad Sci U S A* **121**

24. Ghosh A, Singh J (2024) **Translation initiation or elongation inhibition triggers contrasting effects on Caenorhabditis elegans survival during pathogen infection** *bioRxiv* https://doi.org/10.1101/2024.01.15.575653

25. Gokul G, Singh J (2022) **Dithiothreitol causes toxicity in C. elegans by modulating the methionine-homocysteine cycle** *Elife* **11** https://doi.org/10.7554/eLife.76021

26. Greer EL, Brunet A (2009) **Different dietary restriction regimens extend lifespan by both independent and overlapping genetic pathways in C. elegans** *Aging Cell* **8**:113–127 https://doi.org/10.1111/j.1474-9726.2009.00459.x

27. Guerrero GA *et al.* (2021) **NHR-8 and P-glycoproteins uncouple xenobiotic resistance from longevity in chemosensory C. elegans mutants** *Elife* **10** https://doi.org/10.7554/eLife.53174

28. Hansen M, Chandra A, Mitic LL, Onken B, Driscoll M, Kenyon C (2008) **A role for autophagy in the extension of lifespan by dietary restriction in C. elegans** *PLoS Genet* **4** https://doi.org/10.1371/journal.pgen.0040024

29. Herbst S *et al.* (2015) **Phagocytosis-dependent activation of a TLR 9– BTK–calcineurin–NFAT pathway co-ordinates innate immunity to Aspergillus fumigatus** *EMBO Mol Med* **7**:240–258

30. Hogan PG, Chen L, Nardone J, Rao A (2003) **Transcriptional regulation by calcium, calcineurin, and NFAT** *Genes Dev* **17**:2205–2232 https://doi.org/10.1101/gad.1102703.GENES

31. Jia K, Levine B (2007) **Autophagy is required for dietary restriction-mediated life span extension in C. elegans** *Autophagy* **3**:597–599 https://doi.org/10.4161/auto.4989

32. Johnson TE, De Castro E, de Castro S Hegi, Cypser J, Henderson S, Tedesco P (2001) **Relationship between increased longevity and stress resistance as assessed through gerontogene mutations in Caenorhabditis elegans** *Exp Gerontol* **36**:1609–1617 https://doi.org/10.1016/S0531-5565(01)00144-9

33. Kaeberlein TL, Smith ED, Tsuchiya M, Welton KL, Thomas JH, Fields S, Kennedy BK, Kaeberlein M (2006) **Lifespan extension in Caenorhabditis elegans by complete removal of food** *Aging Cell* **5**:487–494 https://doi.org/10.1111/j.1474-9726.2006.00238.x

34. Kawli T, Wu C, Tan M-W (2010) **Systemic and cell intrinsic roles of Gq signaling in the regulation of innate immunity, oxidative stress, and longevity in Caenorhabditis elegans** *Proc Natl Acad Sci* **107**:13788–13793 https://doi.org/10.1073/pnas.0914715107

35. Kim DH *et al.* (2002) **A Conserved p38 MAP Kinase Pathway in Caenorhabditis elegans Innate Immunity** *Science* **80**:623–626 https://doi.org/10.1126/science.1073759

36. Kim DH, Liberati NT, Mizuno T, Inoue H, Hisamoto N, Matsumoto K, Ausubel FM (2004) **Integration of Caenorhabditis elegans MAPK pathways mediating immunity and stress resistance by MEK-1 MAPK kinase and VHP-1 MAPK phosphatase** *Proc Natl Acad Sci* **101**:10990–10994 https://doi.org/10.1073/pnas.0403546101

37. Klee CB, Ren H, Wang X (1998) **Regulation of the Calmodulin-stimulated Protein Phosphatase, Calcineurin** *J Biol Chem* **273**:13367–13370 https://doi.org/10.1074/jbc.273.22.13367

38. Kuhara A, Inada H, Katsura I, Mori I (2002) **Negative regulation and gain control of sensory neurons by the C. elegans calcineurin TAX-6** *Neuron* **33**:751–763 https://doi.org/10.1016/S0896-6273(02)00607-4

39. Kumar S, Egan BM, Kocsisova Z, Schneider DL, Murphy JT, Diwan A, Kornfeld K (2019) **Lifespan Extension in C. elegans Caused by Bacterial Colonization of the Intestine and Subsequent Activation of an Innate Immune Response** *Dev Cell* **49**:100–117 https://doi.org/10.1016/j.devcel.2019.03.010

40. Labed SA, Wani KA, Jagadeesan S, Hakkim A, Najibi M, Irazoqui JE (2018) **Intestinal Epithelial Wnt Signaling Mediates Acetylcholine-Triggered Host Defense against Infection** *Immunity* **48**:963–978 https://doi.org/10.1016/j.immuni.2018.04.017

41. Lakowski B, Hekimi S (1998) **The genetics of caloric restriction in Caenorhabditis elegans** *Proc Natl Acad Sci U S A* **95**:13091–13096 https://doi.org/10.1073/pnas.95.22.13091

42. Lapierre LR *et al.* (2013) **The TFEB orthologue HLH-30 regulates autophagy and modulates longevity in Caenorhabditis elegans** *Nat Commun* **4** https://doi.org/10.1038/ncomms3267

43. Il Lee J, Mukherjee S, Yoon KH, Dwivedi M, Bandyopadhyay J (2013) **The multiple faces of calcineurin signaling in Caenorhabditis elegans: Development, behaviour and aging** *J Biosci* **38**:417–431 https://doi.org/10.1007/s12038-013-9319-6

44. Lee J, Song HO, Jee C, Vanoaica L, Ahnn J (2005) **Calcineurin regulates enteric muscle contraction through EXP-1, excitatory GABA-gated channel, in C. elegans** *J Mol Biol* **352**:313–318 https://doi.org/10.1016/j.jmb.2005.07.032

45. Lynn DA, Dalton HM, Sowa JN, Wang MC, Soukas AA, Curran SP (2015) **Omega-3 and -6 fatty acids allocate somatic and germline lipids to ensure fitness during nutrient and oxidative stress in Caenorhabditis elegans** *Proc Natl Acad Sci* **112**:15378–15383 https://doi.org/10.1073/pnas.1514012112

46. Magner DB, Wollam J, Shen Y, Hoppe C, Li D, Latza C, Rottiers V, Hutter H, Antebi A (2013) **The NHR-8 nuclear receptor regulates cholesterol and bile acid homeostasis in C. elegans** *Cell Metab* **18**:212–224 https://doi.org/10.1016/j.cmet.2013.07.007

47. Mair W, Morantte I, Rodrigues APC, Manning G, Montminy M, Shaw RJ, Dillin A (2011) **Lifespan extension induced by AMPK and calcineurin is mediated by CRTC-1 and CREB** *Nature* **470**:404–408 https://doi.org/10.1038/nature09706

48. Mallo G V, Le C, Couillault C, Pujol N, Granjeaud S, Kohara Y, Ewbank JJ (2002) **Inducible Antibacterial Defense System in C. elegans** *Curr Biol* **12**:1209–1214

49. Matai L, Chandra G, Chamoli M, Malik Y, Kumar SS, Rautela U, Jana NR, Chakraborty K, Mukhopadhyay A (2019) **Dietary restriction improves proteostasis and increases life span through endoplasmic reticulum hormesis** *Proc Natl Acad Sci* **116**:17383–17392 https://doi.org/10.1073/pnas.1900055116

50. Min S, Oh Y, Verma P, Whitehead SC, Yapici N, Van Vactor D, Suh GSB, Liberles SD (2021) **Control of feeding by piezo-mediated gut mechanosensation in drosophila** *Elife* **10** https://doi.org/10.7554/eLife.63049

51. Morselli E *et al.* (2010) **Caloric restriction and resveratrol promote longevity through the Sirtuin-1-dependent induction of autophagy** *Cell Death Dis* **1** https://doi.org/10.1038/cddis.2009.8

52. Muñoz MJ, Riddle DL (2003) **Positive selection of Caenorhabditis elegans mutants with increased stress resistance and longevity** *Genetics* **163**:171–180 https://doi.org/10.1093/genetics/163.1.171

53. Naim N, Amrit FRG, Ratnappan R, Delbuono N, Loose JA, Ghazi A (2021) **Cell nonautonomous roles of NHR-49 in promoting longevity and innate immunity** *Aging Cell* **20** https://doi.org/10.1111/acel.13413

54. O'Rourke EJ, Ruvkun G (2013) **MXL-3 and HLH-30 transcriptionally link lipolysis and autophagy to nutrient availability** *Nat Cell Biol* **15**:668–676 https://doi.org/10.1038/ncb2741

55. Otarigho B, Aballay A. (2021) **Immunity-longevity tradeoff neurally controlled by GABAergic transcription factor PITX1/UNC-30** *Cell Rep* **35** https://doi.org/10.1016/j.celrep.2021.109187

56. Otarigho B, Aballay A. (2020) **Cholesterol regulates innate immunity via nuclear hormone receptor NHR-8** *iScience* **23** https://doi.org/10.1016/j.isci.2020.101068

57. Panowski SH, Wolff S, Aguilaniu H, Durieux J, Dillin A (2007) **PHA-4/Foxa mediates diet-restriction-induced longevity of C. elegans** *Nature* **447**:550–555 https://doi.org/10.1038/nature05837

58. Ravi Kumar A, Bhattacharyya S, Singh J (2023) **Thiol reductive stress activates the hypoxia response pathway** *EMBO J* **42** https://doi.org/10.15252/embj.2023114093

59. Ren Z, Ambros VR (2015) **Caenorhabditis elegans microRNAs of the let-7 family act in innate immune response circuits and confer robust developmental timing against pathogen stress** *Proc Natl Acad Sci U S A* **112**:E2366–E2375 https://doi.org/10.1073/pnas.1422858112

60. Robida-Stubbs S, Glover-Cutter K, Lamming DW, Mizunuma M, Narasimhan SD, Neumann-Haefelin E, Sabatini DM, Blackwell TK (2012) **TOR signaling and rapamycin influence longevity by regulating SKN-1/Nrf and DAF-16/FoxO** *Cell Metab* **15**:713–724 https://doi.org/10.1016/j.cmet.2012.04.007

61. Santo PD, Logan MA, Chisholm AD, Jorgensen EM (1999) **The inositol triphosphate receptor regulates a 50-second behavioral rhythm in C. elegans** *Cell* **98**:757–767

62. Schulz RA, Yutzey KE (2004) **Calcineurin signaling and NFAT activation in cardiovascular and skeletal muscle development** *Dev Biol* **266**:1–16 https://doi.org/10.1016/j.ydbio.2003.10.008

63. Selman C *et al.* (2009) **Ribosomal Protein S6 Kinase 1 Signaling Regulates Mammalian Life Span** *Science* **80**:140–144

64. Sheng M, Hosseinzadeh A, Muralidharan SV, Gaur R, Selstam E, Tuck S (2015) **Aberrant fat metabolism in Caenorhabditis elegans mutants with defects in the defecation motor program** *PLoS One* **10** https://doi.org/10.1371/journal.pone.0124515

65. Singh J, Aballay A (2019) **Microbial colonization activates an immune fight-and-flight response via neuroendocrine signaling** *Dev Cell* **49**:89–99 https://doi.org/10.1016/j.devcel.2019.02.001

66. Singh J, Aballay A (2019) **Intestinal infection regulates behavior and learning via neuroendocrine signaling** *Elife* **8** https://doi.org/10.7554/eLife.50033

67. Singh J, Aballay A (2019) **Similar Neural Pathways Control Foraging in Mosquitoes and Worms** *MBio* **10**:e00656–19

68. Singh J, Aballay A (2017) **Endoplasmic reticulum stress caused by lipoprotein accumulation suppresses immunity against bacterial pathogens and contributes to immunosenescence** *MBio* **8**:e00778–17 https://doi.org/10.1128/mBio.00778-17

69. Song X, Hu J, Jin P, Chen L, Ma F (2013) **Identification and evolution of an NFAT gene involving Branchiostoma belcheri innate immunity** *Genomics* **102**:355–362 https://doi.org/10.1016/j.ygeno.2013.04.019

70. Soo SK, Traa A, Rudich ZD, Moldakozhayev A, Mistry M, Van Raamsdonk JM (2023) **Genetic basis of enhanced stress resistance in long-lived mutants highlights key role of innate immunity in determining longevity** *Aging Cell* **22** https://doi.org/10.1111/acel.13740

71. Sun J, Singh V, Kajino-Sakamoto R, Aballay A (2011) **Neuronal GPCR Controls Innate Immunity by Regulating Noncanonical Unfolded Protein Response Genes** *Science* **80**:729–732 https://doi.org/10.1126/science.1203411

72. Tao L, Xie Q, Ding YH, Li ST, Peng S, Zhang YP, Tan D, Yuan Z, Dong MQ (2013) **CAMKII and calcineurin regulate the lifespan of caenorhabditis elegans through the FOXO transcription factor DAF-16** *Elife* **2013**:1–23 https://doi.org/10.7554/eLife.00518

73. Teramoto T, Iwasaki K (2006) **Intestinal calcium waves coordinate a behavioral motor program in C. elegans** *Cell Calcium* **40**:319–327 https://doi.org/10.1016/j.ceca.2006.04.009

74. Thomas JH (1990) **Genetic analysis of defecation in Caenorhabditis elegans** *Genetics* **124**:855–872 https://doi.org/10.1016/0168-9525(90)90166-4

75. Thondamal M, Witting M, Schmitt-Kopplin P, Aguilaniu H (2014) **Steroid hormone signalling links reproduction to lifespan in dietary-restricted Caenorhabditis elegans** *Nat Commun* **5** https://doi.org/10.1038/ncomms5879

76. Ulengin-Talkish I, Cyert MS (2023) **A cellular atlas of calcineurin signaling** *Biochim Biophys Acta - Mol Cell Res* **1870** https://doi.org/10.1016/j.bbamcr.2022.119366

77. Vandewalle A, Tourneur E, Bens M, Chassin C, Werts C (2014) **Calcineurin/NFAT signaling and innate host defence: a role for NOD1-mediated phagocytic functions** *Cell Commun Signal* **12**

78. Verma S, Jagtap U, Goyala A, Mukhopadhyay A (2018) **A novel gene-diet pair modulates C. elegans aging** *PLoS Genet* **14** https://doi.org/10.1371/journal.pgen.1007608

79. Wang HD, Kazemi-Esfarjani P, Benzer S (2004) **Multiple-stress analysis for isolation of Drosophila longevity genes** *Proc Natl Acad Sci U S A* **101**:12610–12615 https://doi.org/10.1073/pnas.0404648101

80. Wong A, Boutis P, Hekimi S (1995) **Mutations in the clk-1 gene of Caenorhabditis elegans affect developmental and behavioral timing** *Genetics* **139**:1247–1259 https://doi.org/10.1007/s12020-010-9311-y

81. Xia J, Gravato-Nobre M, Ligoxygakis P (2019) **Convergence of longevity and immunity : lessons from animal models** *Biogerontology* **20**:271–278 https://doi.org/10.1007/s10522-019-09801-w

82. Yee C, Yang W, Hekimi S. (2014) **The intrinsic apoptosis pathway mediates the pro-longevity response to mitochondrial ROS in C. elegans** *Cell* **157**:897–909 https://doi.org/10.1016/j.cell.2014.02.055

83. Zhang Y, Lanjuin A, Chowdhury SR, Mistry M, Silva-garcı CG, Weir HJ, Lee C, Escoubas CC, Tabakovic E, Mair WB (2019) **Neuronal TORC1 modulates longevity via AMPK and cell nonautonomous regulation of mitochondrial dynamics in C. elegans** *Elife* **8**

Editors

Reviewing Editor
Patrick Hu
Vanderbilt University Medical Center, Nashville, United States of America

Senior Editor
Detlef Weigel
Max Planck Institute for Biology Tübingen, Tübingen, Germany

Reviewer #1 (Public review):

In this paper, the authors show that disruption of calcineurin, which is encoded by tax-6 in C. elegans, results in increased susceptibility to P. aeruginosa but extends lifespan. In exploring the mechanisms involved, the authors show that disruption of tax-6 decreases the rate of defecation leading to intestinal accumulation of bacteria and distension of the intestinal lumen. The authors further show that the lifespan extension is dependent on hlh-30, which may be involved in breaking down lipids following deficits in defecation, and nhr-8, whose levels are increased by deficits in defecation. The authors propose a model in which disruption of the defecation motor program is responsible for the effect of calcineurin on pathogen susceptibility and lifespan, but do not exclude the possibility that calcineurin affects these phenotypes independently of defecation.

https://doi.org/10.7554/eLife.89572.2.sa2

Reviewer #2 (Public review):

The relationships between genes and phenotypes are complex and the impact of deleting or a gene can often have multifaceted and unforeseen consequences. This paper dissected the role of calcineurin, encoded by tax-6, in various phenotypes in C. elegans, including lifespan, pathogen susceptibility, the defecation motor program, and nutrient absorption or calorie restriction, through a series of genetic and behavioral analyses. Many genes in these pathways were tested yielding robust results. Classic epistasis analyses were used to distinguish between genes operating in the same or separate pathways. Researchers in the related fields will be very interested in looking through the data presented in this paper in great detail and benefit from it.

Overall, this paper supports a model in which the increased lifespan and heightened pathogen susceptibility observed following calcineurin inhibition result from the disruptions in the defecation motor program but through distinct pathways. A defective defecation motor program leads to intestine bloating and compromised nutrient absorption. Calorie restriction resulting from poor nutrient absorption affects lifespan, whereas increased colonization in the bloated intestine heightens pathogen susceptibility. The observation that knockdown of several other DMP-related genes also results in increased lifespan and pathogen susceptibility further reinforces the proposed model.

https://doi.org/10.7554/eLife.89572.2.sa1

Author response:

The following is the authors' response to the original reviews.

We would like to thank the reviewers for their interest in our studies. In response to their comments, we have conducted additional experiments and made the necessary revisions to the manuscript. The new studies included to address the reviewers' comments are shown in Figure 1B, 1F, Figure 2—figure supplement 1, Figure 3, Figure 3—figure supplement 1, Figure 3—figure supplement 2, Figure 3—figure supplement 3, Figure 4E, Figure 4—figure supplement 1, Figure 5, Figure 5—figure supplement 1, Figure 5—figure supplement 2D, and Figure 6. We are grateful for the critiques, which have helped us substantially improve the quality of the manuscript.

Below, we have provided a point-by-point response to the reviewers' comments.

> ***Public Reviews:***
>
> ***Reviewer #1 (Public Review):***
>
> *In this paper, the authors show that disruption of calcineurin, which is encoded by tax-6 in C. elegans, results in increased susceptibility to P. aeruginosa, but extends lifespan. In exploring the mechanisms involved, the authors show that disruption of tax-6 decreases the rate of defecation leading to intestinal accumulation of bacteria and distension of the intestinal lumen. The authors further show that the lifespan extension is dependent on hlh-30, which may be involved in breaking down lipids following deficits in defecation, and nhr-8, whose levels are increased by deficits in defecation. The authors propose a model in which disruption of the defecation motor program is responsible for the effect of calcineurin on pathogen susceptibility and lifespan, but do not exclude the possibility that calcineurin affects these phenotypes independently of defecation.*

We thank the reviewer for providing an excellent summary of our work. We have performed additional experiments as suggested by both the reviewers and believe we have thoroughly addressed all the reviewers' concerns.

> ***Reviewer #2 (Public Review):***
>
> *The manuscript titled "Calcineurin Inhibition Enhances Caenorhabditis elegans Lifespan by Defecation Defects-Mediated Calorie Restriction and Nuclear Hormone Signaling" by Priyanka Das, Alejandro Aballay, and Jogender Singh reveals that inhibiting calcineurin, a conserved protein phosphatase, in C. elegans affects the defecation motor program (DMP), leading to intestinal bloating and increased susceptibility to bacterial infection. This intestinal bloating mimics calorie restriction, ultimately resulting in an enhanced lifespan. The research identifies the involvement of HLH-30 and NHR-8 proteins in this lifespan enhancement, providing new insights into the role of calcineurin in C. elegans DMP and mechanisms for longevity.*
>
> *The authors present novel findings on the role of calcineurin in regulating the defecation motor program in C. elegans and how its inhibition can lead to lifespan enhancement. The evidence provided is solid with multiple experiments supporting the main claims.*
>
> *Strengths:*
>
> *The manuscript's strength lies in the authors' use of genetic and biochemical techniques to investigate the role of calcineurin in regulating the DMP, innate immunity, and lifespan in C. elegans. Moreover, the authors' findings provide a new mechanism for calcineurin inhibitionmediated longevity extension, which could have significant implications for understanding the molecular basis of aging and developing interventions to promote healthy aging.*

> *(1) The study uncovers a new role for calcineurin in the regulation of C. elegans DMP and a potential novel pathway for enhancing lifespan via calorie restriction involving calcineurin, HLH-30, and NHR-8 in C. elegans.*
>
> *(2) Multiple signaling pathways involved in lifespan enhancement were investigated with fairly strong experimental evidence supporting their claims.*

We thank the reviewer for an excellent summary of our work and for highlighting the strengths of the findings.

> *Weaknesses:*
>
> *The manuscript's weaknesses include the lack of mechanistic details regarding how calcineurin inhibition leads to defects in the DMP and induces calorie restriction-like effects on lifespan.*
>
> *The exact site of calcineurin action, i.e., whether in the intestine or enteric muscles (Lee et al., 2005), and the possible molecular mechanisms linking calcineurin inhibition, DMP defects, and lifespan were not adequately explored. Although characterization of the full mechanism is probably beyond the scope of this paper, given the relative simplicity and advantages of using C. elegans as a model organism for this study, some degree of rigor is expected with additional straightforward control experiments as listed below:*
>
> *The authors state that tax-6 knockdown animals had drastically reduced expulsion events (Figure 2G), leading to irregular DMP (Lines 144-145), but did not describe the nature of DMP irregularity. For example, did the reduced expulsion events still occur with regular intervals but longer cycle lengths? Or was the rhythmicity completely abolished? The former would suggest the intestine clock is still intact, and the latter would indicate that calcineurin is required for the clock to function. Therefore, ethograms of DMP in both wild-type and tax6 mutant animals are warranted to be included in the manuscript. Along the same line, besides the cycle length, the three separable motor steps (aBoc, pBoc, EMC) are easily measurable, with each step indicating where the program goes wrong, hence the site of action, which is precisely the beauty of studying C. elegans DMP. Unfortunately, the authors did not use this opportunity to characterize the exact behavior phenotypes of the tax-6 mutant to guide future investigations. Furthermore, it is interesting that about 64% of tax-6 (p675) animals had normal DMP. The authors attributed this to p675 being a weak allele. It would be informative to further examine tax-6 RNAi as in other experiments or to make a tax-6 null mutant with CRISPR. In addition, in one of the cited papers (Lee et al., 2005), the exact calcineurin loss-of-function strain tax-6(p675) was shown to have normal defecation, including normal EMC, while the gain-of-function mutant of calcineurin tax-6(jh107) had abnormal EMC steps. It wasn't clear from Lee et al., 2005, if the reported "normal defecation" was only referring to the expulsion step or also included the cycle length. Nevertheless, this potential contradiction and calcineurin gain-of-function mutant is highly relevant to the current study and should be further explored as a follow-up to previously reported results. For some of the key experiments, such as tax-6's effects on susceptibility to PA14, DMP, intestinal bloating, and lifespan, additional controls, as the norm of C. elegans studies, including second allele and rescue experiments, would strengthen the authors' claims and conclusions.*

We have now included lifespan, survival on P. aeruginosa, and DMP data using an additional knockout allele, tax-6(ok2065). Additionally, we have added ethograms of DMP for both tax-6 RNAi and the tax-6(ok2065) mutant. Our observations indicate that tax-6 inhibition leads to a complete loss of DMP rhythmicity, suggesting that calcineurin is essential for maintaining the DMP clock. While characterizing the DMP, we noticed that expulsion events appeared

superficial in the tax-6(ok2065) mutant, with little to no gut content released. Consequently, we examined the movement of gut content and found that both tax-6(ok2065) mutants and tax-6 knockdown animals showed significantly reduced gut content movement. The new findings on the characterization of DMP are presented in Figure 2—figure supplement 1, Figure 3, Figure 3—figure supplement 1, and Figure 3—figure supplement 2. The text in the results section reads (lines 160-176): “Next, we investigated whether the reduced number of expulsion events was due to regular intervals with longer cycle lengths or if rhythmicity was entirely disrupted upon tax-6 knockdown. To assess this, we obtained ethograms of the DMP for N2 animals grown on control and tax-6 RNAi. While animals on control RNAi displayed regular cycles of pBoc, aBoc, and EMC, the tax-6 RNAi animals exhibited disrupted rhythmicity (Figure 3A and Figure 3—figure supplement 1). Most tax-6 knockdown animals lacked the pBoc and aBoc steps and had sporadic expulsion events. Isolated pBoc events were occasionally observed, indicating a complete loss of rhythmicity in tax-6 knockdown animals. Ethograms for tax-6(ok2065) animals also showed disrupted rhythmicity (Figure 3B and Figure 3—figure supplement 2). Although the number of expulsion events appeared higher in tax-6(ok2065) animals compared to tax-6 RNAi animals (Figure 3—figure supplement 1 and 2), these expulsion events seemed superficial, releasing little to no gut content. This suggested slow movement of gut content in tax6(ok2065) animals, leading to constipation and intestinal bloating. We examined gut content movement by measuring the clearance of blue dye (erioglaucine disodium salt) from the gut. The clearance was significantly slower in tax-6(ok2065) animals compared to N2 animals (Figure 3C), indicating impaired gut content movement due to the loss of tax-6. Similarly, tax-6 knockdown animals also showed significantly slowed gut content movement (Figure 3D).”

Moreover, we have added a potential reason for the tax-6(p675) contradictory results from Lee et al., 2005 (lines 154-159): “At the 1-day-old adult stage, about 36% of tax-6(p675) animals showed irregular and slowed DMP, while the remainder had regular DMP (Figure 2H), suggesting that tax-6(p675) is a weak allele. The fraction of the animals with irregular DMP appeared to increase with age, indicating that this phenotype might be agedependent. This may also explain why tax-6(p675) animals were reported to have a normal defecation cycle in an earlier study (Lee et al., 2005).”

> *The second weakness of this manuscript is the data presentation for all survival rate curves. The authors stated that three independent experiments or biological replicates were performed for each group but only showed one "representative" curve for each plot. Without seeing all individual datasets or the averaged data with error bars, there is no way to evaluate the variability and consistency of the survival rate reported in this study.*

We now provide all replicates data in the source data files.

> *Overall, the authors' claims and conclusions are justified by their data, but further experiments are needed to confirm their findings and establish the detailed mechanisms underlying the observed effects of calcineurin inhibition on the DMP, calorie restriction, and lifespan in C. elegans.*

We have conducted additional experiments to elucidate the role of calcineurin in the DMP and to investigate the impact of the DMP on calorie restriction and lifespan in C. elegans, as described in the various responses to the reviewers’ comments.

> ***Recommendations for the authors:***
>
> *Our specific comments to guide the authors, should they choose to revise the manuscript:*

> *The RNAi experiments in the eat-2 mutant background are difficult to interpret. If these animals are eating fewer bacteria, it is possible that there is also less tax-6 dsRNA being ingested and therefore less tax-6 inactivation. These experiments should be conducted with a tax-6 null allele.*

We have included lifespan experiments with the eat-2(ad465);tax-6(ok2065) double mutant, along with the individual single mutant controls, as shown in Figure 4E. These results demonstrate that the eat-2 mutation does not further extend the lifespan of the tax-6(ok2065) mutant. Additionally, we confirmed that the eat-2(ad465) mutants do not exhibit defects in feeding-based RNAi (Figure 4—figure supplement 1).

> *While aak-2, hlh-30, and nhr-8 mutants may not have an eat phenotype, the negative tax-6 RNAi results should be confirmed with a tax-6 null mutant to obviate the consideration that these background mutations reduce RNAi efficacy.*

The genes hlh-30 and nhr-8 are located very close to tax-6 on chromosome IV (https://wormbase.org//#012-34-5), which made it challenging to generate double mutants. However, we tested the RNAi sensitivity of the hlh-30(tm1978) and nhr-8(ok186) mutants and confirmed that they are not defective in RNAi (Figure 5—figure supplement 1). We also found that tax-6 RNAi disrupted the DMP in both hlh-30(tm1978) and nhr-8(ok186) mutants (Figure 5—figure supplement 2). Furthermore, our results show that hlh-30(tm1978) and nhr-8(ok186) animals have increased susceptibility to P. aeruginosa upon tax-6 knockdown (Figure 6A, B), indicating that tax-6 RNAi was effective in these mutants. Since the phenotype in the aak-2 mutant was only partially observed, we did not conduct further experiments with aak-2 mutants.

> ***Reviewer #1 (Recommendations For The Authors):***
>
> *The low penetrance of defecation cycle defects in tax-6(p675) worms brings into question the role of the defecation deficits in the phenotypes caused by the disruption of tax6. At the same time, the low penetrance provides a golden opportunity to test this. Do tax6(p675) worms with a normal defecation cycle length have extended longevity? Increased susceptibility to bacterial pathogens? Smaller body size? Distended lumen? Decreased fat accumulation? Increased pha-4 and nhr-8 expression? It would be relatively straightforward to measure defecation cycle length in individual tax-6(p675) worms, bin them into normal defecation and slow defecation groups, and then compare the above-mentioned phenotypes.*

We appreciate the reviewer's interesting suggestion. However, the DMP defect phenotype in tax-6(p675) worms appears to be age-dependent, with the number of DMPdefective worms increasing as they age. Additionally, we observed that exposure to P. aeruginosa accelerates the onset of DMP defects in tax-6(p675) worms. As a result, tax6(p675) worms are not suitable for the type of experiments the reviewer suggested. Nevertheless, we believe that the additional data using the tax-6(ok2065) mutant, along with the characterization of ethograms of DMP, firmly establishes the role of calcineurin in maintaining a regular DMP in C. elegans.

> *Another way to dissect specific effects of calcineurin disruption from phenotypes resulting from defecation motor program deficits would be to further characterize other worms with deficits in defecation (flr-1, nhx-2, pbo-1 RNAi). It is mentioned that they have decreased lifespan. Do they also show increased susceptibility to bacterial pathogens? Do they show decreased fat? Is their lifespan dependent on HLH-30 and NHR-8?*

We thank the reviewer for this important suggestion. We have now included data with flr-1, nhx-2, and pbo-1 RNAi, which shows that the knockdown of these genes also enhances

susceptibility to P. aeruginosa (Figure 3—figure supplement 3G). Knockdown of these genes is already known to reduce fat levels in N2 worms, and we demonstrate that they similarly reduce fat levels in hlh-30(tm1978) and nhr-8(ok186) animals (Figure 5B, C, F, G). Additionally, we found that the increased lifespan observed upon knockdown of these genes (as well as with tax-6 knockdown) is dependent on HLH-30 and NHR-8 (Figure 5A, D).

> *To place "enhanced susceptibility to pathogen" within the proposed model, it would be important to examine the effect of HLH-30 and NHR-8 disruption on this phenotype. The proposed model suggests that this phenotype is independent of HLH-30 and NHR-8, but this should be tested experimentally. Similarly, it would be important to test the effect of HLH-30 and NHR-8 disruption on defecation cycle length to determine if defecation deficits are upstream or downstream of deficits in the defecation motor program*

We show that the knockdown of tax-6 leads to defects in the DMP in hlh30(tm1978) and nhr-8(ok186) animals (Figure 5—figure supplement 2). Moreover, we show that hlh-30(tm1978) and nhr-8(ok186) animals have increased susceptibility to P. aeruginosa upon tax-6 knockdown (Figure 6A, B). These results are described as (lines 279-285): “Given that HLH-30 and NHR-8 are essential for lifespan extension upon calcineurin inhibition, we investigated whether these pathways also influence survival in response to P. aeruginosa infection following calcineurin knockdown. Both hlh-30(tm1978) and nhr-8(ok186) animals showed significantly reduced survival upon tax-6 RNAi (Figure 6A, B). These findings suggested that the reduced survival on P. aeruginosa following calcineurin inhibition is independent of HLH-30 and NHR-8 and is more likely due to increased gut colonization by P. aeruginosa resulting from DMP defects (Figure 6C).”

> *Is the lifespan of tax-6(p675) increased? This would be important to measure and include in Figure 1.*

Indeed, the lifespan of tax-6(p675) mutants is increased. We have included the lifespan of tax-6(p675) and tax-6(ok2065) in Figure 1F.

> *In Figure 2, disruption of tax-6 appears to result in a clear decrease in body size. To what extent is the decrease in fat/worm in Figure 3 simply a result of the worms being smaller? Perhaps, a measurement of Oil-Red-O intensity PER AREA would be a more appropriate measure.*

The ORO intensity values we had shown per animal were already area normalized. We have now indicated this in the Figure Legends.

> *There are multiple long-lived mutant strains such as clk-1 and isp-1 that have an increased defecation cycle length. To what extent do these worms exhibit phenotypes similar to tax-6 disruption? isp-1 have increased resistance to bacterial pathogens suggesting that defecation motor program deficits are not sufficient to increase susceptibility to bacterial pathogens.*

We have now examined the clk-1 and isp-1 mutants and found that these mutants exhibit reduced gut colonization by P. aeruginosa compared to N2 animals. This reduction in colonization may be attributed to the slowed pharyngeal pumping rates observed in these mutants. These findings suggest that the phenotypes associated with a slow DMP versus a disrupted DMP could be significantly different. The manuscript with the new data on these mutants reads (lines 177-192): “We then explored whether the disruption of DMP rhythmicity due to tax-6 knockdown affected P. aeruginosa responses similarly to longer but regular DMP cycles. To do this, we studied P. aeruginosa colonization in clk-1(qm30) and isp1(qm150) mutants, which have regular but extended DMP cycles (Feng et al., 2001; Wong et al., 1995).

Interestingly, both clk-1(qm30) and isp-1(qm150) mutants showed significantly reduced intestinal colonization by P. aeruginosa compared to N2 animals (Figure 3—figure supplement 3A-D). This reduced colonization could be attributed to their significantly decreased pharyngeal pumping rates (Wong et al., 1995; Yee et al., 2014), suggesting a lower intake of bacterial food in these mutants. While the survival of clk-1(qm30) animals on P. aeruginosa was comparable to N2 animals (Figure 3—figure supplement 3E), isp1(qm150) animals exhibited significantly improved survival (Figure 3—figure supplement 3F). Conversely, knockdown of flr-1, nhx-2, and pbo-1 in N2 animals resulted in significantly reduced survival on P. aeruginosa compared to control RNAi (Figure 3—figure supplement 3G). Knockdown of these genes causes complete disruption of DMP rhythmicity, increasing gut colonization by P. aeruginosa (Singh and Aballay, 2019a). Overall, these findings demonstrated that calcineurin is crucial for maintaining the DMP ultradian clock, and its inhibition increases susceptibility to P. aeruginosa by disrupting the DMP."

> *Line 192. This statement is speculative. There is no evidence that HLH-30 is mediating lipid depletion in these worms.*

We have removed this statement. We observed that the knockdown of flr-1, nhx2, and pbo-1 resulted in significant fat depletion in hlh-30(tm1978) animals (Figure 5B, C). Additionally, tax-6 knockdown also caused a small but significant reduction in fat levels in hlh-30(tm1978) animals. This contrasts with our initial submission, possibly due to the increased number of animals included in the analysis. These findings suggest that the increase in lifespan due to DMP defects requires HLH-30, likely through a mechanism independent of HLH-30's role in fat depletion. We have updated the manuscript text and model (Figure 6C) accordingly.

> *In Figure S2, tax-6 RNAi appears to have a more detrimental effect in pmk-1 mutants than the other mutants. The authors should comment on this.*

We have added the following sentence in the manuscript (lines 123-125): "The knockdown of tax-6 appeared to have a more pronounced effect in pmk-1(km25) mutants than in other mutants, suggesting that inhibition of tax-6 might exacerbate the adverse effects observed in pmk-1(km25) mutants."

> ***Reviewer #2 (Recommendations For The Authors):***
>
> *Line 192-193: The statement is confusing and not accurate because HLH-30 did not enhance lifespan with or without calcineurin (Figure 4A and S4A, also in Lapierre 2023). The takeaway should be along the lines of calcineurin inhibition enhancing lifespan through HLH-30 or HLH-30 being required for lifespan enhancement via calcineurin inhibition.*

We have removed this statement. We now state (lines 237-239): "Knockdown of tax-6 did not extend the lifespan of hlh-30(tm1978) animals (Figure 5A), indicating that HLH-30 is required for the increased lifespan observed with calcineurin inhibition."

> *Line 261: Similar to the point above. Where is the data showing NHR-8 increases lifespan with or without calcineurin?*

We have removed this sentence.

> *Figure 1 legend line 699: animals per condition per replicate >90, but in the Method section Line 317, it says more than 80 animals per condition per replicate. Could be more accurate.*

We have now specified in the Methods section that the exact number of animals per condition is provided in the source data files. Since different lifespan curves within a given figure panel had varying numbers of animals, we have indicated the lower boundary for all curves (including the replicates). The precise number of animals for each lifespan experiment is available in the source data files.

> *Figures 2F and G, "tax-6" should be labeled as "tax-6 RNAi" to be consistent with other figures.*

We thank the reviewer for this suggestion and have updated the label to “tax-6 RNAi”.

In summary, we would like to thank the reviewers again for providing constructive critiques. We believe we have fully addressed all the concerns of the reviewers by carrying out several new experiments and modifying the text. The manuscript has undergone substantial revision and has thereby improved significantly. We do hope that the evidence in support of the conclusions is found to be complete in the revised manuscript.

https://doi.org/10.7554/eLife.89572.2.sa0